Coarse graining in time with the functional renormalization group: Relaxation in Brownian motion

Ashley Wilkins [*] and Gerasimos Rigopoulos [†]
School of Mathematics, Statistics and Physics, Newcastle University, Newcastle upon Tyne NE1 7RU, United Kingdom

Enrico Masoero [‡]
Cardiff School of Engineering, Cardiff University Queens Buildings, The Parade, Cardiff CF24 3AA, United Kingdom

(Received 16 June 2022; accepted 13 October 2022; published 3 November 2022)

We apply the functional renormalization group (fRG) to study relaxation in a stochastic process governed by an overdamped Langevin equation with one degree of freedom, exploiting the connection with supersymmetric quantum mechanics in imaginary time. After reviewing the functional integral formulation of the system and its underlying symmetries, including the resulting Ward-Takahashi identities for arbitrary initial conditions, we compute the effective action Γ from the fRG, approximated in terms of the leading and subleading terms in the gradient expansion: the local potential approximation and wave-function renormalization, respectively. This is achieved by coarse graining the thermal fluctuations in time resulting in, e.g., an effective potential incorporating fluctuations at all timescales. We then use the resulting effective equations of motion to describe the decay of the covariance and the relaxation of the average position and variance toward their equilibrium values at different temperatures. We use as examples a simple polynomial potential, an unequal Lennard-Jones type potential, and a more complex potential with multiple trapping wells and barriers. We find that these are all handled well, with the accuracy of the approximations improving as the relaxation's spectral representation shifts to lower eigenvalues, in line with expectations about the validity of the gradient expansion. The spectral representation's range also correlates with temperature, leading to the conclusion that the gradient expansion works better for higher temperatures than lower ones. This paper demonstrates the ability of the fRG to expedite the computation of statistical objects in otherwise long-timescale simulations, acting as a first step to more complicated systems.

DOI: 10.1103/PhysRevE.106.054109

I. INTRODUCTION

Stochastic processes appear in all kinds of contexts in physics: From the Brownian motion (BM) of small particles in a thermal bath [1,2] to exotic scalar fields experiencing quantum fluctuations in the early inflationary universe [3], many problems of interest can be described by the overdamped Langevin Eq. (4). In this paper, we employ an effective description of the stochastic dynamics that captures the aggregate effect of fluctuations embodied in an *effective action* (EA) $\Gamma[\chi(t)]$, a functional of the average position $\chi(t) \equiv \langle x(t) \rangle$ which can be thought of as an analog to the statistical free energy and can be derived from the partition function or generating functional via a Legendre transform. Once obtained, the EA can be used to compute n-point correlation functions of the particle's position $\langle x(t_1)x(t_2)\dots x(t_n)\rangle$, characterizing the system's statistical properties. To obtain this EA, we will be coarse graining the system in time such that we obtain, e.g., an effective potential that incorporates thermal fluctuations on all timescales. To achieve this, we will use a technique known as the functional, or exact, or nonperturbative renormalization group (RG) [4,5]—see Ref. [6] for a review and an entry point to the literature on the subject [7] for a comprehensive overview of applications as well as, e.g., Refs. [8,9] for more elementary introductions.

The RG was brought to full force through the work of Wilson [10], who used it to understand phase transitions, and since then the RG has become a widely used technique in modern physics with many applications in both particle physics [11] and condensed matter physics [12,13]. The RG is relevant whenever fluctuations significantly influence the state (static or dynamical) of a physical system. A recent popular incarnation of this program is the functional RG (fRG) formulation. Wetterich showed [4]—see also Ref. [5]—how one can define Γ at some particular energy or momentum scale Λ in the UV (for us, this will correspond to small time step or high frequency) where the theory is known and then create an RG flow that interpolates through all energy (frequency or momentum) scales down to the IR (i.e., decreasing fluctuation frequency or increasing the characteristic time step of fluctuation here). This change of the effective theory at different scales, the fundamental idea behind the RG, can be formulated in an integrodifferential equation known as the Wetterich equation,

$$k\partial_k\Gamma_k = \tfrac{1}{2}\mathbf{Tr}\left[k\partial_k R_k\left(\Gamma_k^{(2)} + R_k\right)^{-1}\right], \tag{1}$$

[*] a.wilkins3@newcastle.ac.uk
[†] gerasimos.rigopoulos@newcastle.ac.uk
[‡] masoeroe@cardiff.ac.uk

 ©2022 American Physical Society

where Γ_k is the EA at scale k, **Tr** denotes a trace over spatiotemporal points (an integral over spacetime) and a trace over all other relevant indices, R_k is an IR regulator that acts as a cutoff for fluctuations below (momentum or frequency) scale k, and $\Gamma_k^{(2)}$ is the second functional derivative of Γ_k. A simple zero-dimensional manifestation of this flow equation in the context of the Boltzmann equilibrium distribution is illuminating and is reviewed in Appendix A. At the end of the flow, as $k \to 0$, *all* fluctuations are included and the full EA Γ is obtained.

In this paper, we solve Eq. (1) in the context of the dynamics of particles under the influence of a deterministic force, stemming from an arbitrary potential, and thermal fluctuations. We will study a simple polynomial potential, a double Lennard-Jones (LJ) potential, as well as one containing multiple barriers (trapping wells), serving as a toy model of an energy landscape on which particles can diffuse. To solve (1), we employ a widely used approximation scheme, the gradient expansion, to second order. We find good agreement with simulations [and the Fokker-Planck (F-P) equation, where it proved amenable to a numerical solution] at moderate to high temperatures and that this correlates with the spectral representation of the relaxation process, i.e., the overlap between the initial condition (a delta function initial probability distribution) and the spectrum of the F-P operator. In particular, the more the resulting spectrum is shifted toward lower-lying eigenvalues, the better the gradient expansion agrees with the exact evolution. This is in line with expectations about the validity of the gradient expansion, namely, that it better captures slower evolution which should be associated with the lower eigenvalues. Furthermore, we expect that for a fixed initial condition lower temperatures correspond to a spectrum shifted toward higher eigenvalues and, correspondingly, the worst performance of the gradient expansion.

We start in Sec. II by reviewing the connection between Langevin dynamics and supersymmetric quantum mechanics in imaginary time, shown in Ref. [14]—see, e.g., Ref. [15] for a review of this connection. The path integral formulation then allows us to apply the fRG program directly. We include a brief summary of how the Langevin equation can be reformulated in terms of a probability distribution function (PDF) whose evolution is described by the F-P Eq. (32) and how the latter relates to a Euclidean Schrödinger equation. We close the section by discussing the symmetries of the resulting theory and their implications through Ward-Takahashi-type relations, paying attention to the fact that the initial state may not be that of equilibrium.

In Sec. III, we present the flow equations for the EA utilizing a slight modification of the results of Ref. [16] for supersymmetric RG flows. As we explain, the flow equation derived from the supersymmetric formulation ensures compatibility with the equilibrium Boltzmann distribution, a feature not directly obvious from the application of the renormalization group to the Onsager-Machlup form of the generating functional. To turn the functional integrodifferential Eq. (1) into a mathematically more tractable form, we employ two commonly used approximations for the EA Γ_k: the local potential approximation (LPA) as well as the LPA augmented by wave function renormalization (WFR). In the LPA, the effect of fluctuations is progressively taken into account during the flow by the effective potential $V_k(x)$ experienced by the particle, which is altered compared to the bare, fundamental potential $V(x)$. WFR involves a second function $Z_k(x)$, which can be interpreted as a redefinition of position $x \to Z(x)$. These are also known as the first two (leading and subleading) orders in a gradient expansion of Γ.

In Sec. IV, we derive the effective equations of motion (EEOM) through variational derivatives of the EA Γ. We do this first for the one-point function, or average position χ, whose equation of motion simply reduces to an overdamped equation in an effective potential with no noise, i.e., purely classical. We then obtain an equation for the evolution of the two-point function; this Green's function equation allows us to solve for the variance and covariance of the stochastic process. Solutions to these deterministic equations with appropriate initial conditions can then approximate the relaxation toward equilibrium.

In Sec. V, we present numerical solutions to the flow equations for three types of potential: a simple polynomial one, an unequal LJ-type potential, and a rugged potential consisting of an underlying harmonic x^2 potential with the addition of six Gaussian bumps and dips. We also consider different temperatures, effectively controlling the strength of thermal fluctuations compared to the classical force. Naturally, we find that the end results of the flow equations differ, with higher temperatures resulting in potentials that carry less memory of the bare potentials' morphology. In Sec. VI, the numerical solution of the LPA flow equation accurately reproduces static equilibrium quantities, as it should. We also examine the characteristic decay behavior of the connected two-point function $\langle x(0)x(t)\rangle$ or covariance at equilibrium by utilizing both the effective potential $V_{k\to 0}$ and the WFR function $Z_{k\to 0}$ and find good agreement with exact results down to relatively low temperatures when deviations start becoming pronounced.

In Sec. VII, we examine how well the LPA + WFR approximation to the EA can handle relaxation toward equilibrium in our potentials starting from a fixed initial condition $[P_{\rm ini}(x) = \delta(x - x_{\rm ini})]$. Numerical solutions to the EEOM for the one- and two-point functions are compared to direct numerical simulation of Eq. (4) and/or numerical solutions to the FP equation. We find that under the LPA + WFR approximations, the fRG solutions give a good description of the relaxational evolution and are able to capture overshoots of the variance in the potentials we examine. Similarly to equilibrium, the approximations fare worse as the temperature is decreased and the classical force determined by the potential's slope becomes dominant. We suggest that this behavior is correlated to the spectral decomposition of the relaxation in terms of eigenvalues of the relevant FP operator: the more the spectral decomposition of $\langle x(t)\rangle$, $\langle x(t_{\rm ini})x(t)\rangle$, and $\langle x^2(t)\rangle$ is shifted toward lower eigenvalues, the better the LPA + WFR approximation performs.

We conclude in Sec. VIII. Appendix A derives the zero-dimensional analog of the Wetterich Eq. (1) for the effective potential corresponding to the equilibrium Boltzmann distribution while in Appendix B we include a derivation of the solution of (113) that provides the two-point function. In Appendix C, we explicitly show that the determinant appearing in the path integral directly follows from the boundary conditions imposed in Sec. II A.

II. BROWNIAN MOTION AS SUPERSYMMETRIC QUANTUM MECHANICS

This section reviews BM and its path integral formulation in terms of the action functional of supersymmetric quantum mechanics. In the next section, we will exploit this link to derive the RG flow equations.

BM for a single particle of mass m moving in a potential $\bar{V}(x)$, coupled to an external heat bath with temperature T, can be described by the Langevin equation:

$$m\ddot{x} + \gamma\dot{x} = -m\,\partial_x V(x) + f(t), \tag{2}$$

$$\langle f(t)f(t')\rangle = 2D\gamma^2\delta(t-t'), \tag{3}$$

where γ is a frictional coefficient, $f(t)$ is a Gaussian noise term and $V(x)$ is the potential in which the particle moves. $D = k_bT/\gamma$ is the diffusion constant, given so as to match the Boltzmann equilibrium distribution (should an equilibrium state exists). Hereafter, we will be concerned with the overdamped limit,

$$\dot{x} = -\varepsilon\partial_x V(x) + \eta(t), \tag{4}$$

$$\langle \eta(t)\eta(t')\rangle = 2D\delta(t-t'), \tag{5}$$

to which the system settles over a timescale $\varepsilon \equiv m/\gamma$ which we assume to be short. Note that the overdamped equations are a consistent approximation to the full dynamics as long as $\varepsilon^2 V'' \ll 1$.

We will be examining the impact of changing the temperature, and hence changing the strength of the fluctuating force η, on the coarse-grained effective theory. Let us therefore introduce a reference temperature T_0 and a dimensionless parameter Υ which allows us to dial the temperature around T_0. Writing $D = D_0\Upsilon$, we further define dimensionless variables

$$x = \sqrt{2D_0\varepsilon}\,\hat{x}, \quad t = \varepsilon\,\hat{t}, \tag{6}$$

$$V(x) = \frac{2D_0}{\varepsilon}\hat{V}(\hat{x}), \quad \eta(t) = \sqrt{\frac{2D_0}{\varepsilon}}\,\hat{\eta}(\hat{t}), \tag{7}$$

in terms of which the dynamical equation becomes

$$\frac{d\hat{x}}{d\hat{t}} = -\frac{\partial\hat{V}}{\partial\hat{x}} + \hat{\eta}(\hat{t}), \tag{8}$$

$$\langle\hat{\eta}(\hat{t})\hat{\eta}(\hat{t}')\rangle = \Upsilon\delta(\hat{t}-\hat{t}'). \tag{9}$$

From here onward, we will be dropping the hats for simplicity of notation but generally refer to dimensionless quantities unless otherwise stated.

A. The Brownian motion path integral

To bring the tools of quantum field theory [11,17] to bear, we will need to reformulate the stochastic differential Eq. (8) in terms of a path integral. In this subsection, we will outline one known way to obtain this path integral, aiming to link this to supersymmetric quantum mechanics. Our final expression, and the starting point of our subsequent analysis, is the BM transition probability (24), expressed in terms of an integral over possible histories weighted by the action (25), to which the busy reader may progress if uninterested in the details of the derivation. We will be using a condensed functional notation of infinite-dimensional functional integrals but all expressions can be considered as limits of finite, high-dimensional ordinary integrals. This derivation is based on the path integral reformulation by De Dominicis, Peliti, and Janssen [18–20] of the well-known Martin-Siggia-Rose approach for stochastic dynamics, developed in Ref. [21]. More details on these path integrals, including the corresponding finite discretization of the stochastic process, can be found in Ref. [22]—see also Ref. [23] for a pedagogical exposition.

The dynamics of the (dimensionless) Langevin Eq. (8) can be captured in terms of the PDF $\mathcal{P}(x_f|x_i)$ of observing the particle at x_f at time $t = t_f$ given that, initially, at $t = t_i$, the particle was at x_i. By definition, this can be expressed as

$$\mathcal{P}(x_f|x_i) = \langle\delta(x(t_f) - x_f)\rangle, \tag{10}$$

where the expectation value is taken over all possible realizations of the noise $\eta(t)$ and $\delta(x(t_f) - x_f)$ is the Dirac delta function. Put another way, $x(t_f)$ is the position at t_f for a given noise history $\eta(t)$ and the brackets indicate averaging over all possible noise histories, or stochastic paths, which start at x_i and end up at $x(t_f) = x_f$ at t_f. To express this in a path integral form, we can rewrite the PDF using a Gaussian measure for the noise (5) and express the average as

$$\mathcal{P}(x_f|x_i) = \int \mathcal{D}\eta(t)\delta(x(t_f) - x_f)\exp\left[-\int dt\,\frac{\eta^2(t)}{2\Upsilon}\right], \tag{11}$$

where each noise history is weighted by the exponential factor in the above expression. We now consider the identity (see, e.g., Ref. [15]):

$$1 = \int dx_f \int_{x_i}^{x_f} \mathcal{D}x(t)\,\delta(x(t) - x_\eta(t)) \tag{12}$$

$$= \int dx_f \int_{x_i}^{x_f} \mathcal{D}x(t)\,\delta(\dot{x} + V_{,x} - \eta(t))\mathrm{det}\mathbf{M}$$

$$= \int_{x_i} \mathcal{D}x(t)\,\delta(\dot{x} + V_{,x} - \eta(t))\mathrm{det}\mathbf{M}, \tag{13}$$

where the matrix $\mathbf{M}(t,t')$ is

$$\mathbf{M} \equiv \frac{\delta[\dot{x} + V_{,x} - \eta(t)]}{\delta x(t')} = \left(\frac{d}{dt} + V_{,xx}\right)\delta(t-t'). \tag{14}$$

This identity expresses the obvious fact that if the particle starts at some x_i and follows a particular history $x_\eta(t)$ dictated by the Langevin equation without disappearing, it will end up somewhere after time t_f. We have used the standard subscript notation to denote the derivative with respect to that variable, e.g., $V_{,xx} = \partial_{xx}V$. Note that the path integral in (13) is over all paths starting at x_i at t_i and ending at any x at t_f. Inserting this fat unity factor (13) into (11) and noting that the delta function there restricts $x(t_f)$ to be x_f we obtain

$$\mathcal{P}(x_f|x_i) = \int_{x(t_i)=x_i}^{x(t_f)=x_f} \mathcal{D}\eta\mathcal{D}x\,\delta[\dot{x} + V_{,x} - \eta]\,\mathrm{det}\mathbf{M}$$

$$\times\exp\left[-\int dt\,\frac{\eta^2(t)}{2\Upsilon}\right], \tag{15}$$

where the $\mathcal{D}x(t)$ integral is taken over all paths beginning at x_i and ending at x_f. We can rewrite the delta function as a functional Fourier transform using a new variable $\tilde{x}$ which is usually called the response field:

$$\delta[\dot{x} + V_{,x} - \eta] = \int \mathcal{D}\tilde{x} \exp\left[i \int dt\ \tilde{x}(\dot{x} + V_{,x} - \eta) \right]. \quad (16)$$

There are a couple of standard ways we can incorporate det$\mathbf{M}$ into an exponential. We can formally write

$$\mathbf{M} = \left(\frac{d}{dt}\right)\left(1 + \left(\frac{d}{dt}\right)^{-1} V_{,xx}\right) \equiv \left(\frac{d}{dt}\right)\tilde{\mathbf{M}}, \quad (17)$$

where

$$\left(\frac{d}{dt}\right)^{-1}(t, t') = \lambda\Theta(t - t') - (1 - \lambda)\Theta(t' - t). \quad (18)$$

Imposing retarded (causal) boundary conditions, which are appropriate for the problem at hand, requires that we set $\lambda = 1$ and we find

$$\begin{aligned} \det\mathbf{M} &= \det\left(\frac{d}{dt}\right) \times \det\tilde{\mathbf{M}} \propto \exp[\mathrm{Tr}\log(\tilde{\mathbf{M}})] \\ &\propto \exp\left[\frac{1}{2}\int dt\ V_{,xx}\right], \end{aligned} \quad (19)$$

where we used the Stratonovich prescription ($\theta(0) = 1/2$). Alternatively, and to make the link with SuperSymmetry (SUSY), we can use anticommuting Grassmann variables c and $\bar{c}$ such that

$$\det\mathbf{M} = \int \mathcal{D}c\mathcal{D}\bar{c} \exp\left[\int dt\ \bar{c}(\partial_t + V_{,xx})c\right]. \quad (20)$$

The determination of det$\mathbf{M}$ then requires appropriate boundary conditions for $\bar{c}$ and c, which are

$$c(t_{\mathrm{in}}) = 0, \quad \bar{c}(t_{\mathrm{f}}) = 0. \quad (21)$$

Other choices are possible but lead to determinant values that are different from (19), corresponding to noncausal boundary conditions for the stochastic problem. The boundary condition (21) is implied by the discretized form of the path integral, see Ref. [23]. Its appropriateness is verified by direct computation in Appendix C. The discretized path integral can also be consulted to infer that we must further impose

$$\tilde{x}(t_{\mathrm{f}}) = 0. \quad (22)$$

Although introducing c and $\bar{c}$ is not strictly necessary, it pays to keep the determinant expressed in this form since, as we see below, it allows us to conveniently express hidden symmetries of the resulting action. Inserting Eqs. (16) and (20) into (15), we obtain

$$\begin{aligned} \mathcal{P}(x_f|x_i) = \int \mathcal{D}\eta\mathcal{D}x\mathcal{D}\tilde{x}\mathcal{D}c\mathcal{D}\bar{c} \\ \times \exp\left[\int dt \left\{ -\frac{\eta^2}{2\Upsilon} + i\tilde{x}(\dot{x} + V_{,x} - \eta) \right.\right. \\ \left.\left. + \bar{c}(\partial_t + V_{,xx})c \right\}\right]. \end{aligned} \quad (23)$$

We can now trivially perform the Gaussian integral over η to obtain the path integral in terms of the BM action $\mathcal{S}_{\mathrm{BM}}(x, \tilde{x}, \bar{c}, c)$:

$$\mathcal{P}(x_f|x_i) = \int \mathcal{D}x\mathcal{D}\tilde{x}\mathcal{D}c\mathcal{D}\bar{c} \exp[-\mathcal{S}_{\mathrm{BM}}(x, \tilde{x}, \bar{c}, c)], \quad (24)$$

$$\mathcal{S}_{\mathrm{BM}}(x, \tilde{x}, \bar{c}, c) = \int dt \left[\frac{\Upsilon}{2}\tilde{x}^2 - i\tilde{x}(\dot{x} + V_{,x}) - \bar{c}(\partial_t + V_{,xx})c\right]. \quad (25)$$

Computing this path integral, which henceforth shall be called the Brownian path integral, without resorting to some approximation is, in general, impossible analytically. Instead, we will be using numerical solutions to the fRG flow equations to compute it in the LPA + WFR approximations.

Redefining our fields as

$$\begin{aligned} x(t) &\equiv \sqrt{\Upsilon}\,\varphi(t), \\ V(x) &\equiv \Upsilon\, W(\varphi), \\ \tilde{x} &\equiv \frac{1}{\sqrt{\Upsilon}}(i\dot{\varphi} - \tilde{F}), \\ \bar{c}c &\equiv i\bar{\rho}\rho, \end{aligned} \quad (26)$$

we obtain

$$\mathcal{S}_{\mathrm{BM}}[\varphi, \tilde{F}, \bar{\rho}, \rho] = [W(\varphi_f) - W(\varphi_i)] + \mathcal{S}_{\mathrm{SUSY}}, \quad (27)$$

where

$$\begin{aligned} \mathcal{S}_{\mathrm{SUSY}}[\varphi, \tilde{F}, \bar{\rho}, \rho] = \int dt \left[\frac{1}{2}\dot{\varphi}^2 + \frac{1}{2}\tilde{F}^2 + i\tilde{F}W_{,\varphi}(\varphi) \right. \\ \left. - i\bar{\rho}(\partial_t + W_{,\varphi\varphi}(\varphi))\rho\right]. \end{aligned} \quad (28)$$

Action (28) describes the dynamics of Euclidean, or imaginary time, supersymmetric quantum mechanics where ρ and $\bar{\rho}$ are the fermionic fields and φ and $\tilde{F}$ are the bosonic fields [16]. The same action also describes BM and the BM action is equivalent to the SUSY QM one up to a factor depending on the initial and final positions x_i and x_f; these terms can be simply taken outside the path integral as an exponential prefactor.

Variation of $\mathcal{S}_{\mathrm{SUSY}}$ with respect to $\tilde{F}$ yields its equation of motion $\tilde{F} = -iW_{,\varphi}$ which when substituted back into $\mathcal{S}_{\mathrm{SUSY}}$ yields the on mass-shell action

$$\begin{aligned} \mathcal{S}_{\mathrm{OM}}[\varphi, \bar{\rho}, \rho] = \int dt \left[\frac{1}{2}\dot{\varphi}^2 + \frac{1}{2}{W_{,\varphi}}^2 \right. \\ \left. - i\bar{\rho}(\partial_t + W_{,\varphi\varphi})\rho\right]. \end{aligned} \quad (29)$$

We will keep working with the auxiliary field $\tilde{F}$ and (28) as it allows for the symmetry transformations to take on a simpler form, linear in all fields.

It is illuminating to express the above action in terms of the original dimensional variables and perform the integration over $\bar{\rho}$ and ρ, leading to the alternative form of the term

stemming from the determinant:

$$\mathcal{S}_{\rm OM}[x] = \int \frac{dt}{2Dm}\left[\frac{1}{2}m\dot{x}^2 + \frac{1}{2}\varepsilon^2 m V_{,x}{}^2 - Dm\varepsilon V_{,xx}\right] \tag{30}$$

Note that $2Dm$ has the dimensions of action and therefore plays in the thermal problem a role analogous to $\hbar$ in quantum mechanics—see also Sec. II B in this respect. Unlike $\hbar$ of course, it can be varied by changing the temperature, therefore controlling the strength of fluctuations.

B. The Fokker-Planck equation and the spectral expansion

Before moving on to the fRG, we outline the more standard procedure as to how the on-mass shell action (30) can be obtained from the FP equation which resembles a Euclidean Schrödinger equation. We will see later—in Sec. VII D—that the spectral expansion method outlined here confirms the validity of the fRG approach at moderate to high temperatures.

Instead of working with the Langevin equation directly, one can deal with the probability distribution of position:

$$P(x,t) = \langle \delta(x - x_\eta)\rangle, \tag{31}$$

where x_η is the solution to (4) for a given noise function η (i.e., a specific particle trajectory). It can be shown that this evolves according to the following PDE:

$$\frac{\partial P(x,t)}{\partial t} = \partial_x(P(x,t)\partial_x V) + \frac{\Upsilon}{2}\partial_{xx}P(x,t), \tag{32}$$

which is known as the F-P equation. It is usually more useful, however, to rescale the PDF like so:

$$P(x,t) = e^{-V/\Upsilon}\tilde{P}(x,t). \tag{33}$$

This leads to the F-P equation taking the form

$$\frac{\Upsilon}{2}\frac{\partial \tilde{P}(x,t)}{\partial t} = \left(\frac{\Upsilon}{2}\right)^2 \partial_{xx}^2 \tilde{P}(x,t) + \bar{U}\tilde{P}(x,t), \tag{34}$$

$$\bar{U} \equiv \frac{\Upsilon}{4}\partial_{xx}^2 V - \frac{1}{4}(\partial_x V)^2, \tag{35}$$

which resembles a Euclidean Schrödinger equation with $\Upsilon/2$ playing the role of $\hbar$ in controlling the fluctuation amplitude, as one might expect.

Equation (34) can be solved in terms of a spectral expansion (see, e.g., Refs. [2,24]). Writing

$$\tilde{P}(x,t) = \sum_{n=0}^{\infty} c_n p_n(x) e^{-E_n t}, \tag{36}$$

we find that p_n satisfy the corresponding, time-independent Euclidean Schrödinger equation:

$$-\frac{\Upsilon}{2}\frac{d^2 p_n}{dx^2} + \frac{1}{2}\left(\frac{(V_{,x})^2}{\Upsilon} - V_{,xx}\right)p_n = E_n p_n. \tag{37}$$

The lowest eigenfunction with $E_0 = 0$ is

$$p_0(x) = \mathcal{N} e^{-V(x)/\Upsilon}, \tag{38}$$

corresponding to the equilibrium distribution $P_{\rm eq}(x) = p_0(x)^2$. The $p_n(x)$ eigenfunctions are complete and orthonormal:

$$\int_{-\infty}^{\infty} dx\, p_n(x)p_m(x) = \delta_{mn}, \tag{39}$$

$$\sum_{n=1}^{\infty} p_n(x)p_n(x_0) = \delta(x - x_0). \tag{40}$$

The conditional probability, a quantity akin to the evolution operator or propagator in quantum mechanics, can be expressed in terms of the spectral expansion as

$$\tilde{P}(x,t|x_0,0) = \sum_{n=0}^{\infty} p_n(x)p_n(x_0)e^{-E_n t}, \tag{41}$$

$$P(x,t|x_0,0) = e^{-V(x)/\Upsilon}\tilde{P}(x,t|x_0,0)e^{+V(x_0)/\Upsilon}. \tag{42}$$

Any correlation function can then be expressed by using (42). An economic notation can be achieved by using Dirac bra-ket notation in terms of which, e.g.,

$$\tilde{P}(t,0) = \sum_{n=0}^{\infty} |n\rangle e^{-E_n t}\langle n|. \tag{43}$$

Correlation functions can then be expressed in the spectral expansion as

$$\langle f(x(t))g(x(0))\rangle = \sum_{n=0}^{\infty} \langle 0|f|n\rangle e^{-E_n t}\langle n|g|{\rm in}\rangle, \tag{44}$$

where, explicitly,

$$\langle 0|f|n\rangle = \int_{-\infty}^{\infty} dx\, p_0(x)f(x)p_n(x), \tag{45}$$

$$\langle n|g|{\rm in}\rangle = \int_{-\infty}^{\infty} dx\, p_n(x)\, g(x)\tilde{P}(x,0). \tag{46}$$

Note that the out state in the stochastic problem is always $\langle 0|$ and the in state is defined in terms of $\tilde{P}(x, t = 0)$.

We can also write the conditional probability,

$$P(x,t|x_0,0) = \langle x|e^{-V(x)/\Upsilon}\tilde{P}(t,0)e^{+V(x_0)/\Upsilon}|x_0\rangle, \tag{47}$$

governed by the above Euclidean Schrödinger equation, as a path integral,

$$P(x,t|x_0,0) = \mathcal{N}\exp\left(\frac{\varepsilon}{2D}[V(x) - V(x_0)]\right)\int_{x(0)=x_0}^{x(t)=x}\mathcal{D}x(\tau) \times \exp\left(-\int\frac{d\tau}{2Dm}\left\{\frac{1}{2}m(\partial_\tau x)^2 - \bar{U}(x)\right\}\right), \tag{48}$$

where we have reinstated the dimensionful variables. We therefore recover the on mass-shellpath integral (30) obtained earlier. Note the importance of including the determinant (19) in order to obtain the $\partial_{xx}^2 V$ term in the Schrödinger potential $\bar{U}$.

Before proceeding to the next sections, we should add a comment regarding the above path integrals. Beyond being expressions that allow formal manipulations, they can also be understood as limits of large multivariate integrals arising from the discretization of time evolution into small discrete time intervals. In general, this discretization results in apparent ambiguities [25].[1] In our case, this can also be linked to the discretization of the Langevin equation (8) (the index i refers

[1]We would like to thank the anonymous referee for highlighting this point.

to the ith time interval),

$$x_i = x_{i-1} + V'(x_i^\star)\Delta t + \int_{t_{i-1}}^{t_i} ds\, \xi(s), \tag{49}$$

where $x_i^\star = \alpha x_i + (1-\alpha)x_{i-1}$. In the above discussions and manipulations, we have tacitly assumed $\alpha = 1/2$ (Stratonovich) which, in the continuous limit is equivalent to setting $\Theta(0) = 1/2$ [22]. It is well-known, however, that, as long as the noise amplitude does not depend on x (known as additive noise), the solution to the Langevin equation is unique, as is the corresponding F-P equation. Our path integrals respect this and all results derived from them are independent of the choice of α. Calculations with the discrete version, show that contributions from terms involving α cancel. For example, one can start from the discretized path integral with an arbitrary choice of α and obtain a unique F-P equation—see, e.g., Ref. [22]. In the continuum formulation, the supersymmetry discussed in Sec. II D below imposes the cancellation of terms where the ambiguous quantity $\Theta(t=0)$ appears. This is also reflected in the path integral (48) through the special form of the potential $U(x)$ in terms of the superpotential $V(x)$. Overall, this nondependence on α ultimately stems from the inclusion of the determinant det$\mathbf{M}$ in (13). These considerations support the view that the formal path integrals considered here are well-defined and free from any ambiguity.

C. Correlation functions from the generating functional

One way to compute correlation functions is through the use of objects called *generating functionals*. In this subsection, we will outline how these generating functionals yield correlators in practice. We will then outline in Sec. III how the fRG can be used to compute these generating functionals in the first place and therefore how to obtain correlation functions in Sec. IV.

The first generating functional we examine is the partition functional $\mathcal{Z}(\mathrm{J})$, which depends on source terms $\mathrm{J}(t)$ (in analogy with a magnetic field source term $M(x)$ in spin systems),

$$\mathcal{Z}(\mathrm{J}) = \int \mathcal{D}\Phi \exp\left[-\mathcal{S}_{\mathrm{BM}}[\Phi] + \int dt\, \mathrm{J}\Phi\right], \tag{50}$$

which, under variation with respect to J will give any required correlator. In the above functional integral, Φ stands collectively for $(\varphi(t), \tilde{F}(t), \rho(t), \bar{\rho}(t))$ and $\mathrm{J}(t)$ for all the corresponding currents:

$$\int dt\, \mathrm{J}\Phi \equiv \int dt (J_\varphi \varphi + J_{\tilde{F}}\tilde{F} + \bar{\rho}\zeta + \bar{\zeta}\rho). \tag{51}$$

The only constraint we will require of the currents is that they satisfy $\mathrm{J}(t_{\mathrm{in}}) = \mathrm{J}(t_{\mathrm{f}}) = 0$ at the initial and final times t_{in} and t_{f}.

The averages of the fields are defined by

$$\langle \Phi(t)\rangle \equiv \int \mathcal{D}\Phi\ \Phi(t)\ \exp[-\mathcal{S}_{\mathrm{BM}}[\Phi]], \tag{52}$$

$$= \left.\frac{\delta \mathcal{Z}[\mathrm{J}]}{\delta \mathrm{J}(t)}\right|_{\mathrm{J}=0}, \tag{53}$$

the two point correlation function is:

$$\langle \Phi(t_1)\Phi(t_2)\rangle \equiv \frac{\int \mathcal{D}\Phi\ \Phi(t_1)\Phi(t_2)\ \exp[-\mathcal{S}[\Phi]]}{\int \mathcal{D}\Phi \exp[-\mathcal{S}[\Phi]]} \tag{54}$$

$$= \left.\frac{\delta^2 \mathcal{Z}(\mathrm{J})}{\delta \mathrm{J}(t_2)\delta \mathrm{J}(t_1)}\right|_{J=0}, \tag{55}$$

and similarly for higher correlation functions. Note that the usual normalization by a factor $\mathcal{Z}(0)^{-1}$ that is included in general, is omitted here since for this theory $\mathcal{Z}(0) = 1$ by construction.

Defining

$$\mathcal{W}[\mathrm{J}] \equiv \ln(\mathcal{Z}(\mathrm{J})) \tag{56}$$

allows us to compute connected correlation functions (or Ursell functions) as

$$\langle \Phi(t_1)...\Phi(t_n)\rangle_C = \left.\frac{\delta^n \mathcal{W}[\mathrm{J}]}{\delta \mathrm{J}(t_1)...\delta \mathrm{J}(t_n)}\right|_{\mathrm{J}=0}. \tag{57}$$

For instance, the connected two-point function (more commonly known as covariance) $G(t_1, t_2)$ is

$$G(t_1,t_2) \equiv \langle \Phi(t_1)\Phi(t_2)\rangle_C = \langle \Phi(t_1)\Phi(t_2)\rangle - \langle \Phi(t_1)\rangle\langle \Phi(t_2)\rangle$$

$$= \left.\frac{\delta^2 \mathcal{W}[\mathrm{J}]}{\delta \mathrm{J}(t_1)\delta \mathrm{J}(t_2)}\right|_{\mathrm{J}=0}. \tag{58}$$

D. Symmetry transformations for $\mathcal{S}_{\mathrm{BM}}$ and Ward-Takahashi identities

In this subsection, we recall the transformations that leave the action $\mathcal{S}_{\mathrm{BM}}$ invariant, up to boundary terms. We comment on the implications of such symmetries, also paying attention to the boundary terms that are usually dropped under the assumption of equilibrium or, equivalently, a corresponding infinite amount of elapsed time between initial and final states [26]. For us to later use SUSY fRG flow equations in Sec. III, it is crucial to verify the presence of this symmetry in an out-of-equilibrium context.

In general, invariances of the action imply relations between various correlation functions in field theory, generally known as Ward-Takahashi (W-T) identities. Their derivation can be summarized as follows: A general infinitesimal transformation of the fields $\Phi \to \Phi' = \Phi + \Delta\Phi$ will generically change the action $S \to \mathcal{S}' = \mathcal{S} + \Delta\mathcal{S}$. Also shifting $\mathrm{J} \to \mathrm{J} + \Delta\mathrm{J}$ leads to

$$\Delta\mathcal{Z} = \int dt \frac{\delta \mathcal{Z}}{\delta \mathrm{J}(t)}\Delta\mathrm{J}(t) = \int \mathcal{D}\Phi e^{-\mathcal{S}[\Phi]+\int dt\, \mathrm{J}\Phi}$$

$$\times (-\Delta\mathcal{S} + \mathrm{J}\Delta\Phi + \Delta\mathrm{J}\,\Phi), \tag{59}$$

where we used that (a) Φ is simply an integration variable in (50) and $\mathcal{Z}$ is not altered by a change in Φ but only via J and (b) $\mathcal{D}\Phi = \mathcal{D}\Phi'$, i.e., the transformation involves no nontrivial Jacobian determinant. Symmetries of the dynamical system comprise transformations for which ΔS is, at most, a total derivative (or a total divergence for higher dimensions): $\Delta\mathcal{S} = \int dt \frac{d}{dt}\mathcal{A} = \mathcal{A}(t_f) - \mathcal{A}(t_i) = [\mathcal{A}]_{t_i}^{t_f}$. Further choosing $\Delta\mathrm{J}$ such that, for a given $\Delta\Phi$, $\mathrm{J}\Delta\Phi + \Delta\mathrm{J}\,\Phi = 0$, leads to

$$\int dt \frac{\delta \mathcal{Z}}{\delta \mathrm{J}(t)}\Delta\mathrm{J}(t) = \int \mathcal{D}\Phi[\mathcal{A}]_{t_i}^{t_f} e^{-\mathcal{S}[\Phi]+\int dt\, \mathrm{J}\Phi}. \tag{60}$$

Differentiating this master equation with respect to J and setting $\mathrm{J} = 0$, gives relations between correlations functions that are necessitated by the symmetry under $\Phi \to \Phi + \Delta\Phi$.

For our case, given two independent, infinitesimal Grassmann variables ϵ and $\bar{\epsilon}$, the following transformations of the fields [16]:

$$\varphi \to \varphi + i\bar{\epsilon}\rho - i\bar{\rho}\epsilon, \tag{61}$$

$$\tilde{F} \to \tilde{F} - \bar{\epsilon}\dot{\rho} - \dot{\bar{\rho}}\epsilon, \tag{62}$$

$$\rho \to \rho + (\dot{\varphi} - i\tilde{F})\epsilon, \tag{63}$$

$$\bar{\rho} \to \bar{\rho} + \bar{\epsilon}(\dot{\varphi} + i\tilde{F}), \tag{64}$$

leave $\mathcal{S}_{\mathrm{BM}}$ invariant up to a boundary term at the initial time t_{in}:

$$\mathcal{S}_{\mathrm{BM}} \to \mathcal{S}_{\mathrm{BM}} + \bar{\rho}_{\mathrm{in}}(i\dot{\varphi} + \tilde{F} + 2iW_{,\varphi})_{\mathrm{in}}\epsilon, \tag{65}$$

where subscript in denotes the initial time t_{in}. The boundary term at t_{f} has been eliminated using the boundary condition (21). Note that the $\bar{\epsilon}$ transformation leaves $\mathcal{S}_{\mathrm{BM}}$ invariant identically, irrespective of the boundary conditions.

Adding source currents $(J_\varphi,\ J_{\tilde{F}},\ \zeta, \bar{\zeta})$ to the action [27]

$$\mathcal{S}_{\mathrm{BM}} \to \mathcal{S}_{\mathrm{BM}} - \int dt (J_\varphi \varphi + J_{\tilde{F}}\tilde{F} + \bar{\rho}\zeta + \bar{\zeta}\rho) \tag{66}$$

and requiring appropriate transformations of those currents,

$$J_\varphi \to J_\varphi + \dot{\bar{\zeta}}\epsilon + \bar{\epsilon}\dot{\zeta}, \tag{67}$$

$$J_{\tilde{F}} \to J_{\tilde{F}} + i\bar{\zeta}\epsilon - i\bar{\epsilon}\zeta, \tag{68}$$

$$\zeta \to \zeta + \epsilon(iJ_\varphi - \dot{J}_{\tilde{F}}), \tag{69}$$

$$\bar{\zeta} \to \bar{\zeta} - \bar{\epsilon}(iJ_\varphi + \dot{J}_{\tilde{F}}), \tag{70}$$

we have

$$\mathrm{J}\Phi \to \mathrm{J}\Phi - \bar{\epsilon}\frac{d}{dt}(\rho J_{\tilde{F}} - \varphi\zeta) - \frac{d}{dt}(\bar{\rho}J_{\tilde{F}} - \varphi\bar{\zeta})\epsilon. \tag{71}$$

We therefore see that the transformations result in

$$\mathcal{S}_{\mathrm{BM}} - \mathrm{J}\Phi \to \mathcal{S}_{\mathrm{BM}} - \mathrm{J}\Phi + \bar{\rho}_{\mathrm{in}}(i\dot{\varphi} + \tilde{F} + 2iW_{,\varphi})_{\mathrm{in}}\epsilon \tag{72}$$

and the exponent in the integrand of (50) only changes by a lower boundary term that is also independent of $\bar{\epsilon}$.

The field transformation (61)–(64) are linear shifts that leave the integration measure in the path integral invariant. Coupled with the shift in the currents we find, setting $\epsilon = 0$,

$$\int dt \left[\frac{\delta\mathcal{Z}}{\delta J_\varphi(t)}\dot{\zeta} - i\frac{\delta\mathcal{Z}}{\delta J_{\tilde{F}}(t)}\zeta - \frac{\delta\mathcal{Z}}{\delta\bar{\zeta}(t)}(iJ_\varphi + \dot{J}_{\tilde{F}})\right] = 0, \tag{73}$$

while for $\bar{\epsilon} = 0$ we obtain

$$\int dt \left[\frac{\delta\mathcal{Z}}{\delta J_\varphi(t)}\dot{\bar{\zeta}} + i\frac{\delta\mathcal{Z}}{\delta J_{\tilde{F}}(t)}\bar{\zeta} - \frac{\delta\mathcal{Z}}{\delta\zeta(t)}(iJ_\varphi - \dot{J}_{\tilde{F}})\right]$$
$$= \int \mathcal{D}\Phi[-\bar{\rho}_{\mathrm{in}}(i\dot{\varphi}_{\mathrm{in}} + \tilde{F}_{\mathrm{in}} + 2iW'_{\mathrm{in}})]e^{-\mathcal{S}_{\mathrm{BM}} + \int dt\,\mathrm{J}\Phi}. \tag{74}$$

These are the master equations from which so-called Ward-Takahashi identities between various correlators can be obtained. For example, differentiating (73) with respect to $J_\varphi(t')$, $\zeta(\tau)$ and setting $\mathrm{J} = 0$ gives

$$\frac{d}{d\tau}\langle\varphi(t')\varphi(\tau)\rangle + \langle\varphi(t')W'(\varphi(\tau))\rangle - i\langle\rho(t')\bar{\rho}(\tau)\rangle = 0, \tag{75}$$

which, along with the original Langevin equation, allows us to infer that

$$i\langle\rho(t')\bar{\rho}(\tau)\rangle = \frac{1}{\sqrt{\Upsilon}}\langle\varphi(t)\eta(\tau)\rangle, \tag{76}$$

meaning that $\langle\rho(t')\bar{\rho}(\tau)\rangle$ is proportional to the response of $\varphi(t')$ to noise $\eta(\tau)$ (clearly a retarded quantity $\propto\Theta(t'-\tau)$). Furthermore, Eq. (75) can be rewritten as

$$\sqrt{\Upsilon}\langle\tilde{x}(\tau)\varphi(t')\rangle = -\langle\bar{\rho}(\tau)\rho(t')\rangle, \tag{77}$$

which confirms that $\langle\varphi(t')\tilde{x}(\tau)\rangle$ is the retarded response function or propagator. Importantly, Eq. (77) also establishes that in a diagrammatic expansion, closed ghost loops act to cancel closed loops involving the retarded propagator. This ensures $\mathcal{Z}[\mathrm{J} = 0] = 1$, which simply reflects conservation of probability, and furthermore that correlators do not depend on the ill-defined quantity $\Theta(0)$, reflecting the well-known fact that, for additive noise, the discretization of the stochastic differential equation (Ito, Stratonovic, etc.) does not matter.

Differentiating (74) with respect to $J_\varphi(t')$, $\bar{\zeta}(\tau)$ and setting $\mathrm{J} = 0$ gives, with the use of (77) and recalling that integration over $\tilde{F}$ gives $\tilde{F} \to -iW_{,\varphi}$,

$$2\frac{d}{d\tau}\langle\varphi(t')\varphi(\tau)\rangle - i\sqrt{\Upsilon}\langle\tilde{x}(\tau)\varphi(t')\rangle + i\sqrt{\Upsilon}\langle\tilde{x}(t')\varphi(\tau)\rangle$$
$$= -i\Upsilon\langle\tilde{x}_{\mathrm{in}}\varphi(\tau)\rangle\langle\tilde{x}_{\mathrm{in}}\varphi(t')\rangle. \tag{78}$$

This is a modified Fluctuation-Dissipation relation with the term on the right-hand side accounting for the initial condition. Sending $t_{\mathrm{in}} \to -\infty$ makes the right-hand side vanish and we recover the Fluctuation-Dissipation relation at equilibrium [26]:

$$\frac{d}{d\tau}\langle\varphi(t')\varphi(\tau)\rangle = i\frac{\sqrt{\Upsilon}}{2}(\langle\tilde{x}(\tau)\varphi(t')\rangle - \langle\tilde{x}(t')\varphi(\tau)\rangle). \tag{79}$$

III. APPLYING THE FUNCTIONAL RENORMALIZATION GROUP

The functional renormalization group (fRG) has already been applied to study nonequilibrium physics, see, e.g., Refs. [28–39] for an incomplete selection of references. Recently, the fRG has further been used for averaging fluctuations in the *temporal domain* of Langevin dynamics in Ref. [40] but without direct use of the supersymmetry. As discussed in Ref. [41], the physically inspired conditions the authors of Ref. [40] require of their flow equations are straightforwardly imposed by the supersymmetric flow. The Supersymmetric flow equation itself was first derived in Ref. [16] but without making any connection to stochastic dynamics. This connection was made independently in Ref. [35]—see also Ref. [27]—which, however, considered a field theory in extended spatial dimensions and smoothing the corresponding *spatial fluctuations*, not temporal fluctuations as we do here. In fact, the authors of Ref. [16] obtained a slightly different flow equation when WFR is included since

they do not connect the action functional they study to BM and the corresponding equilibrium Boltzamnn distribution. This Supersymmetric fRG flow has only been very recently utilized in the context of stochastic dynamics in early universe inflation [41–43].

The formulation of the fRG involves the Wetterich equation [4], which is a functional (infinite dimensional) integrodifferential equation describing the flow of the EA between the microscopic and macroscopic scale. This flow is controlled by a parameter k that ranges from the UV cutoff Λ down to the IR regime as $k \to 0$. In our BM scenario, microscopic regime refers to a small time step and macroscopic to a long time step. The definition of $\Lambda \sim 1/\Delta t$ is analogous to the condensed matter interpretation of the cutoff being inversely proportional to the lattice size, the only difference here being that the condensed matter lattice is in space and ours is in time. We will use the fRG ultimately to calculate correlation functions of the particle position. As this derivation uses known techniques and results, we refer the busy reader to our basic equations and main results of this section: Eq. (88) for the LPA to the RG flow and when we also include WFR, they are (95) and (96).

The fRG formulation adds a regulating term to the action in our definition of the generating functional:

$$\mathcal{Z}_k(J) = \int \mathcal{D}\Phi \exp\left[-\mathcal{S}[\Phi] - \Delta\mathcal{S}_k[\Phi] + \int_t \mathrm{J}\Phi\right], \tag{80}$$

where the regulating term $\Delta\mathcal{S}_k[\Phi]$ is quadratic in Φ:

$$\Delta\mathcal{S}_k[\Phi] = \frac{1}{2}\int_{t,t'} \Phi(t) R_k(t,t') \Phi(t'). \tag{81}$$

Crucially R_k is an IR regulator that depends on a renormalization scale k and the momentum (frequency) p of the modes. The precise form of R_k is not crucially important and it is chosen to optimize calculations but it should suppress IR modes and vanish as $k \to 0$, $\lim_{k\to 0} R_k = 0$, ensuring that the full EA is recovered in this limit. By defining the mean field as $X(t) \equiv \langle \Phi(t) \rangle$, we can construct the regulated EA,

$$\Gamma_k[X] = \int_t \mathrm{J}X - \mathcal{W}_k[\mathrm{J}] - \Delta\mathcal{S}_k[X], \tag{82}$$

where $\mathcal{W}_k[\mathrm{J}] = \ln(\mathcal{Z}_k)$ and X refers to all the relevant mean fields.

From the regulated EA, one can obtain the Wetterich equation [4,5],

$$\partial_k \Gamma_k[X] = \frac{1}{2}\,\mathrm{STr}\left\{\int_{t,t'} \partial_k R_k(t,t')\left[R_k + \Gamma_k^{(2)}\right]^{-1}\right\}, \tag{83}$$

which is a functional equation determining how Γ_k changes as $k \to 0$. $\Gamma^{(2)}$ is the second functional derivative with respect to the relevant fields and STr refers to the supertrace—see Ref. [16] for details. The equation evolves Γ_k from the microscopic scale ($k = \Lambda$), where $\Gamma_\Lambda = \mathcal{S}$, down to the IR regime ($k = 0$), where the full EA $\Gamma[\chi] = \Gamma_{k=0}[\chi]$, encoding the effect of all fluctuations, is obtained. A simplified derivation for one degree of freedom at equilibrium, which, however, captures all the relevant manipulations, can be found in Appendix A.

As demonstrated in the previous section, our BM problem is actually SUSY QM. We can therefore apply the fRG technology and incorporate the effect of thermal fluctuations by following the flow of the EA Γ_k via the Wetterich equation. Synatschke *et al.* have analyzed a system with action $\mathcal{S}_{\mathrm{SUSY}}$ in light of its underlying symmetries in Ref. [16]—see also Ref. [35]. We adopt their results here. They find that from a supersymmetric perspective, the appropriate regulating term takes the form

$$\begin{aligned}\Delta\mathcal{S}_k = &\int_{\tau\tau'} r_2(k,\Delta\tau)[-\dot\phi(\tau)\dot\phi(\tau') + F(\tau)F(\tau') - i\bar\psi(\tau)\dot\psi(\tau')] \\ &+ 2i r_1(k,\Delta\tau)[\phi(\tau)F(\tau') - \bar\psi(\tau)\psi(\tau')],\end{aligned} \tag{84}$$

where $\Delta\tau \equiv \tau - \tau'$. Such a form was also suggested in Ref. [40], however, we will see that compatibility with the Boltzmann distribution suggests setting $r_2 \to 0$. The flow equations of Ref. [16] are discussed below.

A. Local potential approximation

In practice, calculating Γ_k exactly is usually impossible and we must consider a truncation to make the functional Eq. (83) tractable. The most common approximation is the so-called derivative expansion. The LPA, the leading order in the derivative expansion, is the assumption that the only part of the EA that depends on our momentum scale k is the superpotential W. The EA then takes the form

$$\begin{aligned}\Gamma_k[\phi, F, \bar\psi, \psi] = \int d\tau \Big[&\frac{1}{2}\dot\phi^2 + \frac{1}{2}F^2 + iFW_{k,\phi}(\phi) \\ &- i\bar\psi(\partial_t + W_{k,\phi\phi})\psi\Big],\end{aligned} \tag{85}$$

such that $\Gamma_{k=\Lambda} = \mathcal{S}_{\mathrm{SUSY}}$ under the condition $W_{k=\Lambda}(\phi) = W(\phi)$ with

$$\phi \equiv \langle\varphi\rangle, \quad F \equiv \langle\tilde F\rangle \quad \psi \equiv \langle\rho\rangle, \quad \bar\psi \equiv \langle\bar\rho\rangle \tag{86}$$

are the mean fields, and we also denote $\chi \equiv \langle x\rangle = \sqrt{\Upsilon}\phi$. In this approximation, the only thing changing with k directly, progressively incorporating the effect of fluctuations on different timescales, is W_k. This means we only have one flow equation to solve which turns out to be [16]

$$\partial_k W_k(\phi) = \int_{-\infty}^{\infty} \frac{dp}{4\pi} \frac{(1+r_2)\partial_k r_1 - \partial_k r_2\left(r_1 + \partial_\phi^2 W_k(\phi)\right)}{p^2 + \left(r_1 + \partial_\phi^2 W_k(\phi)\right)^2}.$$

We notice that if we set $r_2 = 0$ and choose a local-in-time $r_1(k, \tau - \tau') = k\delta(\tau - \tau')$, the so-called Callan-Symanzik regulator, then this choice[2] effectively adds a quadratic term to the potential $W \to W + k\phi^2$ and leads to a relatively simple flow equation:

$$\partial_k W_k(\phi) = \frac{1}{4}\frac{1}{k + \partial_\phi^2 W_k(\phi)}. \tag{87}$$

[2]Physically speaking, the final results should be independent of the regulator chosen. This is a subtlety we will not address in this paper, as it was shown in Ref. [16] that even for other choices of regulators the difference in the final results was negligible, at least for the LPA.

In terms of the physical variables, we have

$$\partial_k V_k(\chi) = \frac{\Upsilon}{4}\frac{1}{k + \partial_\chi^2 V_k(\chi)}, \tag{88}$$

which shows explicitly the effect of dialling the temperature Υ: the higher the temperature, the faster the flow as a result of stronger thermal fluctuations. Equation (88) can be discretized in the χ direction and become a set of coupled ODEs that can be solved in the k direction to obtain a numerical solution.

It is important to note that Eq. (88) is identical to the flow of the effective potential that corresponds to the equilibrium Boltzmann distribution, se Ref. [44] and Appendix C with $R \to k$. We therefore see that the form of $\mathcal{S}_{\rm SUSY}$ and deriving flow equations that respect its symmetries establishes automatic consistency with the equilibrium Boltzmann distribution. If one started directly from the Onsager-Machlup functional (30) and naively treated it as an $N = 1$ Euclidean scalar theory in one-dimension with the combination $U = \frac{1}{2}(V_{,x})^2 - \frac{\Upsilon}{2}V_{,xx}$ as the scalar potential to be evolved along the RG flow, one would have obtained a different flow equations:

$$\partial_k U_k(\phi) = \frac{1}{2}\int_{-\infty}^{\infty}\frac{dp}{2\pi}\frac{\partial_k R_k}{p^2 + R_k + \partial_\phi^2 U_k(\phi)}. \tag{89}$$

The corresponding Callan-Symanzik regulator would be $R_k = k^2$, giving

$$\partial_k U_k(\phi) = \frac{1}{2}\frac{k}{\sqrt{k^2 + \partial_\phi^2 U_k(\phi)}}. \tag{90}$$

It is unclear how or if the end-of-the-flow potential $U_{k=0}$ from this equation would relate to the physical potential $V_{k=0}$.

B. Wave function renormalization

In the previous subsection, we assumed that the EA Γ_k only depends on the renormalization scale through the form of the potential. We now allow for the field φ itself to be renormalized, which results in a scaling of the kinetic term. The new EA in the SUSY formalism is [16]

$$\begin{aligned}\Gamma_k[\phi, \bar\psi, \psi] = \int dt\ &\frac{1}{2}Z_{,\phi}^2\dot\phi^2 + \frac{1}{2}\left(\frac{W_{,\phi}}{Z_{,\phi}}\right)^2 \\ &- i\bar\psi\Big(Z_{,\phi}^2\partial_t + Z_{,\phi}Z_{,\phi\phi}\dot\phi \\ &- Z_{,\phi\phi}\frac{W_{,\phi}}{Z_{,\phi}} + W_{,\phi\phi}\Big)\psi,\end{aligned} \tag{91}$$

where we have suppressed the explicit dependence on k of W and Z to avoid overly cluttered notation. From now on, we will, in general, drop this explicit dependence on k for W, V, Z, and ζ, defined below, only restoring it when we are directly comparing it to the original cutoff value. We introduce another identification[3] in addition to (26)

$$\zeta(x) = \sqrt{\Upsilon}Z(\phi) \Rightarrow \zeta_{,x} = Z_{,\phi}, \tag{92}$$

$$\bar c c = -i\zeta_{,x}\bar\psi\psi, \tag{93}$$

such that the (on-shell) EA for BM is now written as

$$\begin{aligned}\Gamma_k[\chi, \bar c, c] = \int dt\ &\frac{1}{2\Upsilon}\zeta_{,\chi}^2\dot\chi^2 + \frac{1}{2\Upsilon}\left(\frac{V_{,\chi}}{\zeta_{,\chi}}\right)^2 \\ &- \bar c\Big(\zeta_{,\chi}^2\partial_t + \zeta_{,\chi}\zeta_{,\chi\chi}\dot\chi \\ &- \zeta_{,\chi\chi}\frac{V_{,\chi}}{\zeta_{,\chi}} + \cdot V_{,\chi\chi}\Big)c.\end{aligned} \tag{94}$$

The regulator term becomes more complicated for this action and we do not reproduce it here, see Ref. [16] for details of this. Following their approach, one arrives at the LPA + WFR flow equations:

$$\partial_k V_k(\chi) = \frac{\Upsilon}{4}\frac{1}{k + \partial_{\chi\chi}^2 V_k(\chi)}, \tag{95}$$

$$\partial_k \zeta_{,\chi} = \frac{\Upsilon}{4}\frac{\mathcal{P}}{\zeta_{,\chi}\cdot\mathcal{D}^2}, \tag{96}$$

$$\mathcal{D} \equiv V_{,\chi\chi} + k\,\zeta_{,\chi}^2, \tag{97}$$

$$\mathcal{P} \equiv \frac{4\zeta_{,\chi\chi}V_{,\chi\chi\chi}}{\mathcal{D}} - (\zeta_{,\chi\chi}\zeta_{,\chi})_{,\chi} - \frac{3\zeta_{,\chi}^2 V_{,\chi\chi\chi}^2}{4\mathcal{D}^2}, \tag{98}$$

which now consist of the previous LPA equation for the effective potential (88) as expected, augmented by one more flow equation for the WFR $\zeta_{,\chi}$.

As before, we will integrate the LPA Eq. (88) by discretizing along the χ direction and solving the resulting set of coupled ODEs in k. Once the effective potential $V_k(\chi)$ has been obtained, the second PDE can be solved for $\zeta_{,\chi}$ in a similar way. It is worth pointing out here that our approach differs slightly from Ref. [16] in that the effective potential obeys the same equation as in the LPA approximation even with the inclusion of WFR.[4] This is because the equilibrium state is described exactly by the LPA equation [43–45], as we mentioned above and explicitly recall in Appendix A. The LPA flow equation was first solved in Refs. [16,44,45], while more recently WFR was included for a double-well potential in Ref. [43].

IV. THE EFFECTIVE EQUATIONS OF MOTION

A standard formulation of classical mechanics involves the principle of least action. If one considers the classical action $\mathcal{S}$,

$$\mathcal{S} = \int dt\ (L(x, \dot x) - jx), \tag{99}$$

[3]This ζ is unrelated to the one appearing in (51).

[4]For the WFR approximation, the authors of Ref. [16] use a spectrally adjusted regulator which is evaluated on a background field $\bar\phi$. They make the simple choice of identifying this background field with the fluctuation field (i.e., $\bar\phi = \phi$). This approach, however, modifies the flow of V_k: Eq. (95) differs from the LPA version (88) and the flow no longer correctly approaches the Boltzmann equilibrium distribution's effective potential. In the approach of Ref. [45], which uses a simplified version of the WFR, this can be corrected by a further rescaling of k.

where $L(x, \dot{x})$ is the Lagrangian and a source term has been added, one can obtain the equations of motion by requiring the variational derivative of $\mathcal{S}$ to be zero:

$$\frac{\delta \mathcal{S}}{\delta x} = j. \tag{100}$$

The EA Γ is so named because its definition makes it look like a classical action but includes the effect of fluctuations that have been integrated out. Defining

$$e^{\mathcal{W}[\mathrm{J}]} = \int \mathcal{D}\Phi \, e^{-\mathcal{S}[\Phi]+\int dt \mathrm{J}\Phi}, \tag{101}$$

the EA $\Gamma[X]$ is then defined as

$$\Gamma[X] = \int_t \mathrm{J}X - \mathcal{W}[\mathrm{J}] \tag{102}$$

where

$$X = \langle \Phi \rangle. \tag{103}$$

We then have

$$\frac{\delta \Gamma}{\delta X} = \mathrm{J}. \tag{104}$$

Therefore Γ, the central object of the fRG, leads to EEOM that incorporate the aggregate effects of the thermal fluctuations.[5]

A. The EEOM for the one-point function

In a similar way to how the classical action $\mathcal{S}(x)$ can yield the classical equations of motion through variational derivatives, so too does $\Gamma[\chi]$ yield the *effective equation of motion* for the one point function (or average position) χ:

$$\frac{\delta \Gamma}{\delta \chi(t)} = 0. \tag{105}$$

Here we have assumed there are no external sources[6] ($\mathrm{J} = 0$). Under the LPA equation (105) is

$$\frac{\delta \Gamma_{k=0}}{\delta \chi(t)} = \ddot{\chi} - \partial_\chi V_{k=0}(\chi)\, \partial_\chi^2 V_{k=0}(\chi) = 0, \tag{106}$$

where the final equality comes by assuming that source terms have been set to zero (i.e., $J(t) = 0$). The WFR version of (105) reads

$$(\zeta_{,\chi}\dot{\chi})^{\cdot} - \frac{\partial_\chi V_{k=0}}{\zeta_{,\chi}^2}\left(\partial_{\chi\chi}^2 V_{k=0} - \frac{\zeta_{,\chi\chi}}{\zeta_{,\chi}}\partial_\chi V_{k=0}\right) = 0, \tag{107}$$

where $\partial_\chi \zeta$ and $\partial_\chi^2 \zeta$ are also evaluated at $k = 0$. Both of these second-order differential equations can actually be reduced to a first-order differential equation like so,

$$\dot{\chi} = -\tilde{V}_{,\chi}(\chi), \tag{108}$$

where we have introduced the *effective dynamical potential* $\tilde{V}$ defined by

$$\tilde{V}_{,\chi}(\chi) \equiv \begin{cases} V_{,\chi}(k=0,\chi), & \text{for LPA} \\ \frac{V_{,\chi}(k=0,\chi)}{\zeta^2_{,\chi}(k=0,\chi)}, & \text{for WFR.} \end{cases} \tag{109}$$

Here we can clearly see that for LPA the *effective* and *effective dynamical* potentials are equivalent whereas WFR provides an additional factor for the latter.

Equation (108) tells us that the equation of motion for the average position χ is an extremely simple first-order differential equation that appears like a Langevin equation with no noise. This means that once you have obtained the *effective dynamical* potential, you can compute the evolution of the average position χ trivially from any starting position.

At equilibrium, the average position of the particle should not change; this means that $\dot{\chi} = 0$. It naturally follows from this condition and the EEOM for χ (108) that equilibrium is defined for both LPA and WFR by the condition

$$\partial_\chi V_{k=0}(\chi_{\mathrm{eq}}) = 0. \tag{110}$$

As the potential $V_{k=0}(\chi)$ should be convex (by definition of Γ) Eq. (127) tells us that χ_{eq} corresponds to the minimum of $V_{k=0}(\chi)$. Or, more concretely:

$$\lim_{t\to\infty} \langle x(t) \rangle = x \text{ that minimises } V_{k=0}(x). \tag{111}$$

The equilibrium position is obviously the same for both LPA and WFR as they both lead to the same effective potential. As the equilibrium position is straightforwardly computed from the Boltzmann distribution, verifying that the minimum of the effective potential matches the predicted equilibrium position is a good first test for the numerical solution of $V_{k=0}(x)$, at least close to its minimum.

B. The EEOM for the two-point function

The connected two-point function $G(t,t') = \langle x(t)x(t')\rangle_C = \delta^2\mathcal{W}/\delta J(t)\delta J(t')$ and the second functional derivative of the EA $\Gamma_{k=0}$ are inverse to each other:

$$\int d\tau \, \frac{\delta^2 \Gamma_{k=0}}{\delta\chi(t)\delta\chi(\tau)} \frac{\delta^2 \mathcal{W}_{k=0}}{\delta J(\tau)\delta J(t')} = \delta(t-t'). \tag{112}$$

Concretely, this means that the connected two-point function $G(t,t')$ satisfies the following equation:

$$\left(\frac{d^2}{dt^2} - \mathcal{U}(\chi(t))\right) G(t,t') = -2\Delta\delta(t-t'), \tag{113}$$

where $\mathcal{U}(\chi)$ is

$$\mathcal{U}(\chi) = \begin{cases} V_{,\chi\chi}^2 + V_{,\chi}V_{,\chi\chi\chi}, & \text{for LPA} \\ \frac{V_{,\chi\chi}^2}{\zeta_{,\chi}^4} + \frac{V_{,\chi}V_{,\chi\chi\chi}}{\zeta_{,\chi}^4} - \frac{V_{,\chi}^2\zeta_{,\chi\chi\chi}}{\zeta_{,\chi}^5} - \frac{5V_{,\chi}V_{,\chi\chi}\zeta_{,\chi\chi}}{\zeta_{,\chi}^5} + \frac{5V_{,\chi}^2\zeta_{,\chi\chi}^2}{\zeta_{,\chi}^6}, & \text{for WFR} \end{cases} \tag{114}$$

[5]These equations are equivalent to those obtained by the 1-PI generating functional [13].

[6]Note that this is not the same as assuming that the noise term (5) is zero, as this is true for Γ by definition.

and

$$\Delta \equiv \begin{cases} \frac{\Upsilon}{2}, & \text{for LPA} \\ \frac{\Upsilon}{2\zeta_\chi^2}, & \text{for WFR.} \end{cases} \tag{115}$$

The derivation of the full solution to (113) can be found in Appendix B but here we just highlight the two main results:

The EEOM for the *variance* $t' \to t$,

$$\mathbf{Var}(x) \equiv G(t,t) = \frac{\Upsilon}{2\lambda P(t)} \tilde{Y}_1(t)\tilde{Y}_2(t) + \frac{P(0)}{P(t)}\left[G_{00} - \frac{\Upsilon}{2\lambda P(0)}\right]\tilde{Y}_2^2(t), \tag{116}$$

and the EEOM for the *covariance* $t' \to 0, t > 0$,

$$\mathbf{Cov}(x(0)x(t)) \equiv G(t,0) = G_{00}\tilde{Y}_2(t), \tag{117}$$

where $\tilde{Y}_i(t) \equiv Y_i(t)/Y_i(0)$ are the normalized solutions to the homogeneous Eq. (B2), which can be obtained numerically. $P(t) = 1$ or $\zeta_\chi(\chi(t))$ for LPA and WFR, respectively, and λ is defined below by (119). $G_{00} = G(0,0)$ is the initial variance at $t = 0$

If we take the equilibrium limit $\chi \to \chi_{\rm eq}$ of the full EEOM for the two-point function (113), we find that it simplifies to

$$\left(\frac{d^2}{dt^2} - \lambda^2\right) G_{\rm eq}(t_1,t_2) = -2\Delta|\delta(t_2 - t_1), \tag{118}$$

where

$$\lambda^2 \equiv \begin{cases} V^2_{,\chi\chi}|, & \text{for LPA} \\ \frac{V^2_{,\chi\chi}|}{\zeta^4_{,\chi}|}, & \text{for WFR,} \end{cases} \tag{119}$$

and Δ is defined as in (115). The notation $|$ means we have evaluated the function at $k = 0$ and at equilibrium $\chi = \chi_{\rm eq}$.

The appropriate solution to (118) providing the connected correlation function at equilibrium is

$$G_{\rm eq}(t_1,t_2) = \mathbf{Cov}_{\rm eq}(x(t_1)x(t_2)) = \frac{\Upsilon}{2V_{,\chi\chi}|} e^{-\lambda|t_1 - t_2|} \tag{120}$$

$$\Rightarrow G_{\rm eq}(t,t) = \mathbf{Var}_{\rm eq}(x) = \frac{\Upsilon}{2V_{,\chi\chi}|}. \tag{121}$$

As the equilibrium variance is also easily computed from the Boltzmann distribution, Eq. (121) gives us a second test to verify that the effective potential has been computed correctly, at least around the minimum.

In the LPA approximation, the variance and the decay rate of the autocorrelation function are both directly given by the curvature of the effective potential at its minimum. The inclusion of WFR, however, alters the decay rate without changing the equilibrium variance. This is as it should be since the latter is fixed by the equilibrium Boltzmann distribution. As we will see, WFR improves the decay rate which is indeed not exactly determined by the effective potential's curvature alone.

V. SOLUTIONS TO THE FLOW EQUATIONS

In this section, we obtain the resulting effective potential and WFR for three types of potential. The first we consider is a simple polynomial in line with [16]

$$V(x) = 1 + x + \frac{x^2}{2} + \frac{2x^3}{3} + \frac{x^4}{4}. \tag{122}$$

We will also consider a double well made by two LJ potentials back to back:

$$V(x) = 4\epsilon_1\left(\frac{\sigma^{12}}{(x+3)^{12}} - \frac{\sigma^6}{(x+3)^6}\right) + 4\epsilon_2\left(\frac{\sigma^{12}}{(x-3)^{12}} - \frac{\sigma^6}{(x-3)^6}\right), \tag{123}$$

where σ will be taken to be 1 from here on in and ϵ_1 and ϵ_2 represent the depth of each well. We will choose $\epsilon_1 = 1$, $\epsilon_2 = 10$, meaning the left well is one unit deep and the right well is ten units deep (in $2D_0/\varepsilon$ units) and the potential is asymmetric. Clearly, here the domain of interest is $x \in (-3,3)$ as the potential diverges at $x = \pm 3$.

Finally, we also consider a bumpy bare potential consisting of a simple x^2 underlying potential with additional Gaussian bumps (or dips),

$$V(x) = x^2 + \sum_{i=1}^{n} \alpha_i \exp\left[-\frac{(x-\beta_i)^2}{\mu}\right], \tag{124}$$

where there are n bumps or dips with the prefactor α_i being positive or negative, respectively. We will focus on an x^2 plus three bumps and three dips in an asymmetrical setup. This potential could represent a rudimentary toy model for motion over a potential energy landscape with a series of local energy minima. This serves to clearly demonstrate the effect of local extrema on the final shape of the effective potential since the underlying x^2 potential does not alter its shape under the RG flow. We chose the parameters to be for x^2 + six bumps or dips:

$$\begin{aligned} &\alpha_1 = \alpha_4 = \alpha_5 = -1.5, \\ &\alpha_2 = \alpha_3 = \alpha_6 = 1.5, \quad \mu = 0.06, \\ &\beta_1 = -\beta_2 = 0.7, \quad \beta_3 = -\beta_4 = 1.4, \quad \beta_5 = -\beta_6 = 2.1, \end{aligned} \tag{125}$$

expressed in dimensionless units (we have set $\hat{x} \to x$ to avoid notational clutter).

We solve the LPA flow Eq. (88) on a grid in the χ direction and use an adaptive step size Runge-Kutta ODE solver to evolve in the k direction. A similar approach was used for including (96). The numerical derivatives in the χ direction were based on a finite difference scheme using the Fornberg method with a stencil size of 5 for the potentials under study. While increasing the grid size improves the accuracy of the numerical derivative, it also increases the number of coupled ODEs to be solved, making the integration much more computationally expensive. A balance must be drawn, depending on the potential in question. For our cases, we considered 1001 points and $x \in (-3,3)$ for the unequal LJ potential and $x \in (-5,5)$ for the other two. Figures 1–5 display the results.

Figures 1 and 2 show the flow from the bare to the effective potential for a high, $\Upsilon = 10$, and a low, $\Upsilon = 1$, temperature for the polynomial and unequal LJ potentials, respectively. As $k \to 0$ is approached, a distinct single minimum develops, indicating the average position of the particle. As expected, the lower the temperature, the closer the effective minimum is to the bare potential's global minimum, reflecting the relative weakness of fluctuations to force the particle to spend time

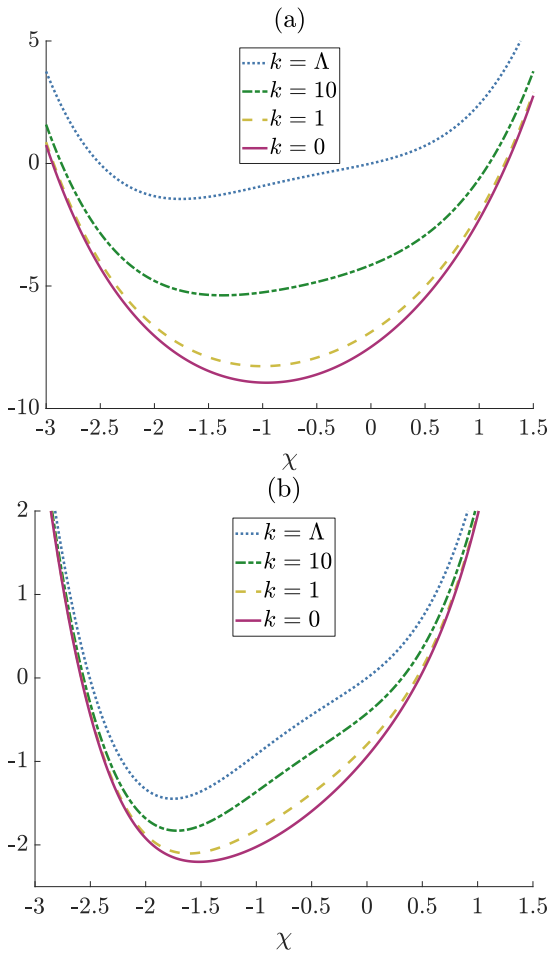

FIG. 1. The flow of the polynomial Langevin potential V in the LPA for (a) $\Upsilon = 10$ [high temperature (strong fluctuations)] and (b) $\Upsilon = 1$ [low temperature (weak fluctuations)]. The dotted blue curve indicates the bare potential which is progressively changed, through dot-dashed green and dashed yellow, into the solid red, effective potential, as fluctuations are integrated out.

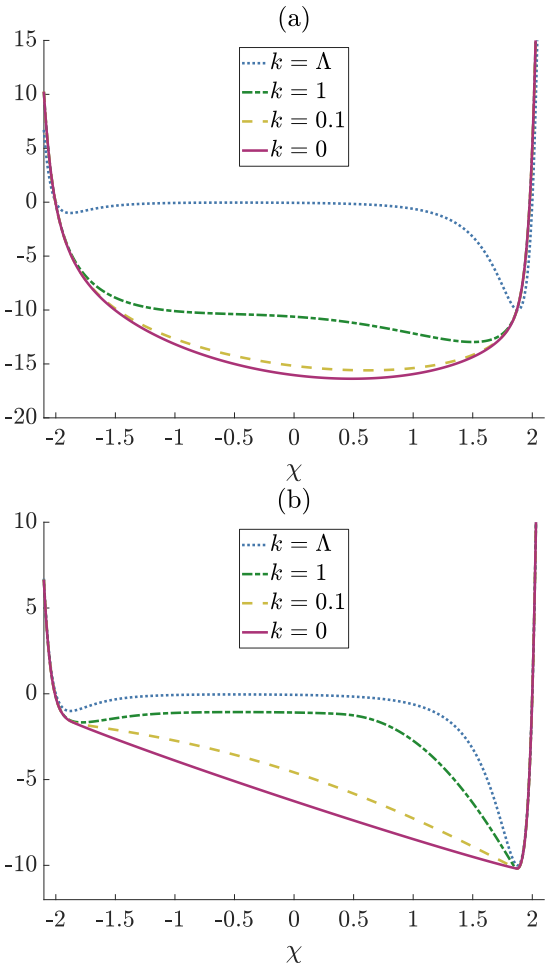

FIG. 2. The flow of the unequal LJ Langevin potential V in the LPA for (a) $\Upsilon = 10$ and (b) $\Upsilon = 1$. Again, the bare potential is denoted by the dotted blue curve and the $k = 0$ effective potential by the solid red one.

away from it. As one might expect, it takes longer in k evolution for local features—e.g., barriers—to disappear in the $\Upsilon = 1$ case as fluctuations at each k scale have less energy than their equivalent for the $\Upsilon = 10$ case and the particle's stochastic motion between barriers is less frequent. Physically, this means that the fluctuations we have integrated out up to scale k do not contribute significantly to the particle moving between minima.

We see a similar phenomenon in Fig. 3 for the flow from the bare to the effective potential for $\Upsilon = 3$, and $\Upsilon = 1$ for an x^2 potential with six Gaussian bumps (dips). Here the original Langevin potential is much more complicated than in the previous two cases but the fRG is still able to smooth out these features in a nontrivial way. This example further demonstrates how the flow of the effective potential is driven by the local curvature, the Gaussian features imposed here, since for an x^2 potential the fRG flow Eq. (88) yields no change beyond an unphysical shift by an overall additive constant.

It is clear in all three figures that at high temperature there is not much change in the shape of the potential when k has reached the value given by the green, dot-dashed line. Physically, this means that the fluctuations integrated out in this range do not contribute significantly to the particle evolution and transition between minima. However, by the time k has been lowered to the value of the yellow, dashed line, we have started to integrate over fluctuations over timescales relevant for interminima transitions. Naturally, when $k = 0$ is reached, the potential is fully convex (as it must be by definition of Γ) with no local features to overcome. Similar behavior is obtained where again we consider the corresponding lower temperature. As one might expect, it takes onger in k evolution for the barrier to disappear as fluctuations at each k scale have less energy than their equivalent for the high temperature case. Of note is that not only is the evolution different but the final shape of $V_{k=0}(x)$ is different for the two different temperature regimes. Both the position and gradient near the global minimum are changed. This is suggestive of longer timescales required at lower temperatures to reach equilibrium. It also indicates longer times for the equilibrium covariance to decay, as we discuss below.

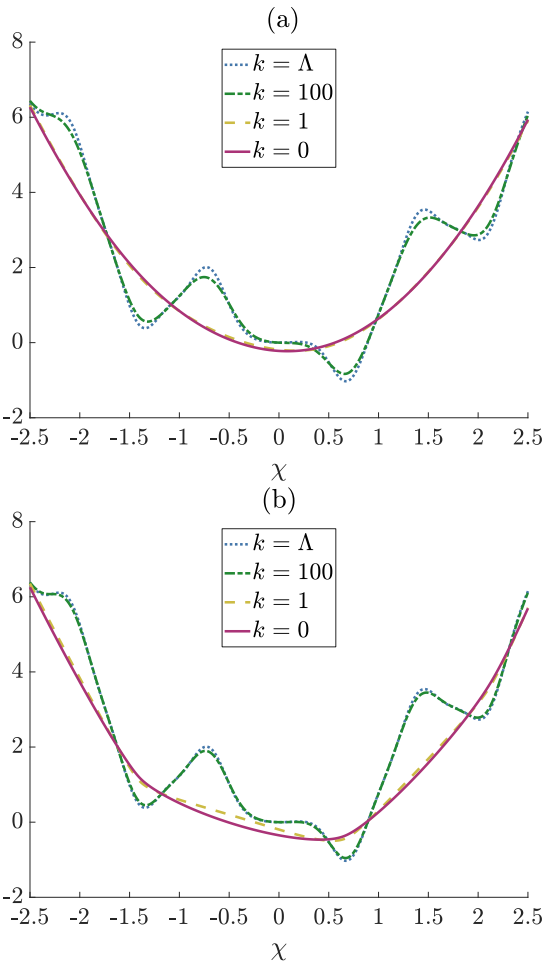

FIG. 3. The flow of the x^2 potential with three additional Gaussian bumps and three dips in the LPA for (a) $\Upsilon = 3$ and (b) $\Upsilon = 1$. As before, the bare potential is denoted by the dotted blue curve and the $k = 0$ effective potential by the solid red one.

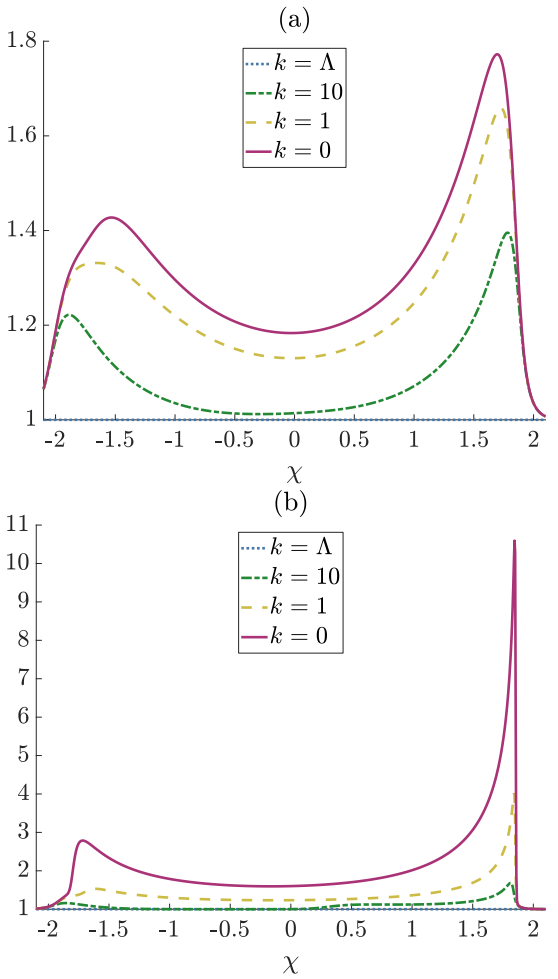

FIG. 4. The flow of ζ_x for of the unequal LJ Langevin potential for (a) $\Upsilon = 10$ and (b) $\Upsilon = 2$.

Regarding WFR, the full numerical solutions to (96) for the unequal L-J potential at $\Upsilon = 10,\ 2$ and for an x^2 potential with six Gaussian bumps (dips) at $\Upsilon = 3$ are shown in Figs. 4 and 5, respectively. We see that from the initial condition, $\zeta_x = 1$ everywhere, features appear as $k \to 0$ in direct contrast with the evolution of the effective potential. At higher temperatures, it is clear that at $k = 0$ a local minima appears at the same place as the global minimum for the effective potential where the height of the local minima is linked to the equilibrium covariance—see Eq. (119). Looking at Fig. 4(b), however, we can see that this is no longer the case and the features generated by the fRG flow are much greater than in the high-temperature case. We will see later that the neighboring features in ζ_x will help to better describe dynamical evolution than the bare potential alone.

VI. EQUILIBRIUM

As mentioned above and recalled in Appendix A, the LPA flow Eq. (88) exactly corresponds to the effective potential of the equilibrium Boltzmann distribution

$$P(x) = N\exp\left(-\frac{2V(x)}{\Upsilon}\right). \tag{126}$$

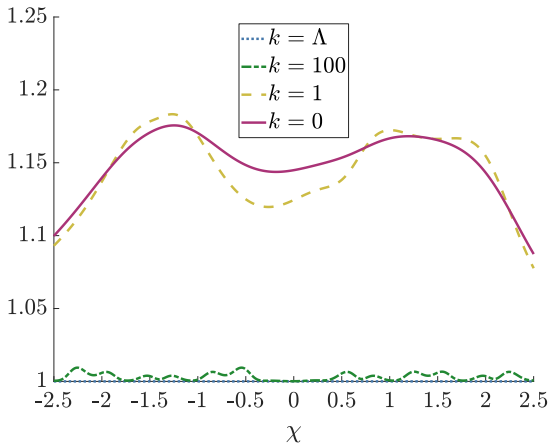

FIG. 5. The flow of ζ_x for an x^2 potential with six Gaussian bumps/dips for $\Upsilon = 3$.

TABLE I. Value of the autocorrelation decay rate at different temperatures. The LPA and WFR columns display λ as calculated from the fRG flow. The simulation values were generated by averaging over 50 000 runs.

Potentials	ϒ	LPA	WFR	Sim
Poly	10	3.1857	2.9101	2.9191
	4	2.0842	1.8664	1.8767
	1	1.7112	1.3381	1.3585
Unequal LJ	10	2.9655	2.0146	1.8783
	2	50.93	0.4806	0.3691
x^2+ 6 b (d)	3	1.9199	1.4529	1.3977
	2	1.8185	1.1552	0.9710

We have verified that both the equilibrium position, given by the minimum of the effective potential,

$$\partial_\chi V_{k=0}(\chi_{\rm eq}) = 0, \tag{127}$$

and the equilibrium variance, defined from the effective potential's curvature through

$$\mathbf{Var}_{\rm eq}(x) = \frac{\Upsilon}{2V_{,\chi\chi}|}, \tag{128}$$

are reproduced to subpercent accuracy, indicating the accuracy of the numerical solution to the LPA flow equation, at least around the minimum of the effective potential.

In addition to the static variance at equilibrium, the curvature of the effective potential around the minimum also determines the time dependence of correlations in equilibrium, quantified by the time-dependent covariance or connected two-point function:

$$\mathbf{Cov}_{\rm eq}(x(t_1)x(t_2)) = \frac{\Upsilon}{2V_{,\chi\chi}|} e^{-\lambda|t_1-t_2|}. \tag{129}$$

Here, λ corresponds to $V_{,\chi\chi}|$ within the LPA but the solution to the WFR flow equation (96) for $\zeta_{,\chi}$ also contributes, providing a correction to λ according to (119).

In Table I, we collect the values of λ obtained using the fRG under LPA and WFR for different ϒ values, and compare this directly to high-accuracy numerical simulations of the Langevin Eq. (4). We can clearly see from Table I that the LPA can have good agreement with the simulation value for simple potentials at high temperature but can deviate drastically as temperature is lowered. Inclusion of the WFR factor ζ_x reduces the deviation error from the value obtained in the simulations substantially to ∼1% for the simplest cases and order of magnitude agreement for the most complicated, low-temperature systems.

The decay of the equilibrium covariance is shown in Figs. 6 and 7 for the polynomial and x^2 plus six bumps (dips) potentials, respectively. We can see—for the polynomial potential—in Fig. 6(a), ϒ = 10, that the LPA and WFR are both in good agreement with simulations and in Fig. 6(b), ϒ = 1, that the WFR offers better agreement than the LPA. In Fig. 7(a), we can see that for ϒ = 3 the WFR prediction closely matches the simulations, offering significant improvement over the LPA, which closely matches the bare x^2 potential. This indicates that even for highly nontrivial systems—where the computation of eigenvalues for these

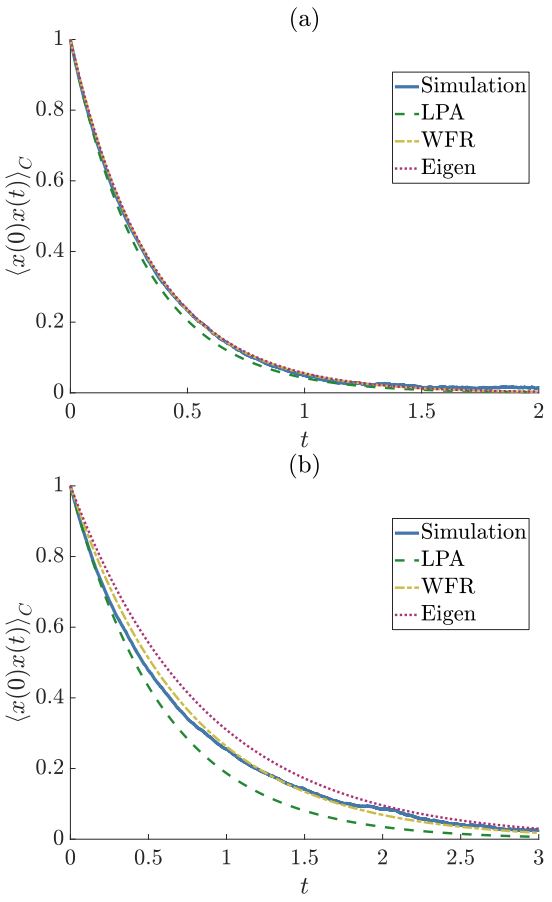

FIG. 6. The decay of the (normalized) covariance $\langle x(0)x(t)\rangle_C$ at equilibrium in a polynomial potential for (a) ϒ = 10 and (b) ϒ = 1.

potentials is a nontrivial exercise—that the simulated decay is vastly different from the bare x^2 potential—see Table I and compare to the x^2 prediction for λ/2 which is 1—the fRG can appropriately capture these effects.

It is also worth pointing out that the simulated decay rate does not follow a pure exponential at all times in all cases. This can be best seen in the top plot of Fig. 6(b), where the decay is initially close to the LPA, then the WFR decay before moving toward the eigen decay rate at late times. This sort of behavior has been identified in similar systems in the early universe [46], where it was noticed that the smallest nonzero eigenvalue's spectral coefficient was sufficiently small that higher order eigenvalues would dominate the decay at earlier times, as LPA matches the decay rate predicted by the Boltzmann distribution and WFR is closer to the decay predicted by E_1. We discuss this further below.

VII. RELAXATION TOWARDS EQUILIBRIUM

To solve the equations of motion for the one point function $\chi(t)$ and two point function $G(t,t')$ we must first solve the PDEs for the LPA and WFR to obtain the *dynamical effective potential* $\tilde{V}$ and the function $\mathcal{U}$. We will use the solutions obtained in Sec. V to compute these parameters and then solve the appropriate EEOM.

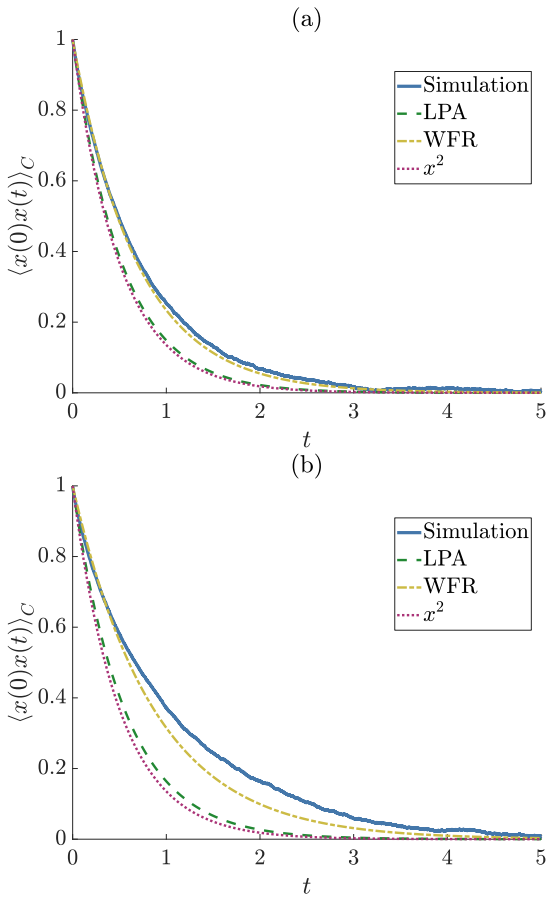

FIG. 7. The decay of the (normalized) covariance $\langle x(0)x(t)\rangle_C$ at equilibrium in an x^2 plus six Gaussian bumps (dips) potential for (a) $\Upsilon = 3$ and (b) $\Upsilon = 2$.

A. The dynamical effective potentials

In Sec. IV, we introduced the notion of the *dynamical effective potential* $\tilde{V}$ given by Eq. (109) which together with (108) describes the evolution of the average position, χ. As the fRG guarantees that the fully effective potential V will be convex, this implies that the dynamical effective potential $\tilde{V}$ will also be either fully or extremely close to fully convex for LPA and WFR, respectively, thus greatly simplifying dynamical calculations. In the previous section, we emphasized how the fRG LPA effective potential gives us the Boltzmann equilibrium quantities such as equilibrium position and variance. What we would like to emphasize now, however, is that away from the minimum of the effective potential the fRG gives us information that the near-equilibrium Boltzmann assumption does not. To be concrete, an approximate Gaussian Boltzmann distribution would assume that the potential is of the form

$$\tilde{V}_{\text{Boltz}}(x) = \frac{\Upsilon}{4 \times \text{Var}_{\text{eq}}}(\chi - \chi_{\text{eq}})^2 \tag{130}$$

where χ_{eq} and Var_{eq} are the equilibrium position and variance, respectively. We show in Fig. 8 how this approximation can break down dramatically as one moves away from the equilibrium position, suggesting that the fRG captures the far away from equilibrium dynamics well. In principle, one could attempt to include higher order cumulants of the Boltzmann distribution such as skewness and kurtosis into an approximate effective potential, however, the relationship between these cumulants and higher derivatives of the effective potential is nontrivial and cumbersome to include. In any case, it is not expected that including these corrections would lead to significant improvement away from equilibrium.

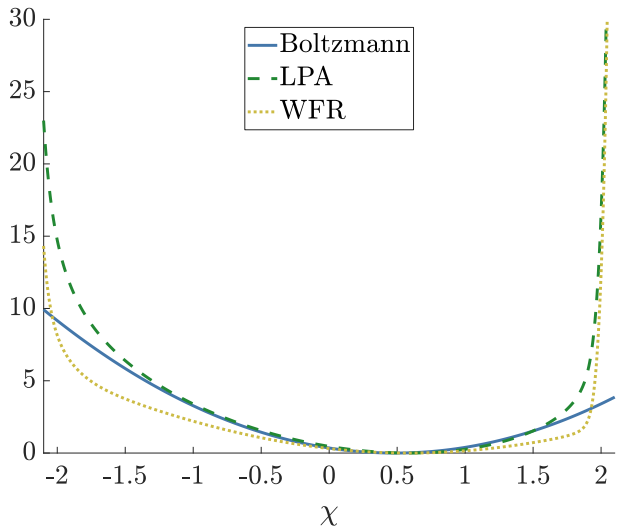

FIG. 8. Comparison of $\tilde{V}$ for unequal LJ potential at $\Upsilon = 10$ as calculated using fRG methods LPA and WFR compared to the Boltzmann near-equilibrium approximation given by Eq. (130). All potentials have been vertically shifted so their minima (corresponding to the equilibrium position) coincide.

B. Accelerated trajectories

Having solved the appropriate flow equations to obtain the dynamical effective potentials, we can now solve (108). Given the dynamical effective potential $\tilde{V}$, it only takes a couple seconds to obtain the full trajectory of χ from some initial position $x_i = \chi_i$ to the equilibrium position. For the polynomial potential, we initialized the particle far away from the equilibrium position at $x = 4$. In Fig. 9, we show how the average position of the particle changes with time using direct simulation of the Langevin Eq. (4) over 50 000 runs by numerically solving the F-P Eq, (34) and as calculated by the evolution in the dynamical effective potentials $\tilde{V}$ given using the LPA and WFR methods at $\Upsilon = 10$. All four trajectories agree to a very high precision.

In Fig. 10, we plot the evolution of $\chi(t)$ for the unequal LJ potential where the particle begins in the smaller well at $x = -1.878$ and moves toward its equilibrium position. We see as before that the WFR trajectory closely matches the simulated trajectory, offering significant improvement over the LPA computation. Note that for this system it was impossible to get convergent numerics for the evolution of the F-P Eq. (34) This ability of the fRG to capture the nontrivial evolution of average position is also shown in Fig. 11 for the x^2 potential plus six bumps (dips), which is a much more complex potential landscape at three different temperatures. Here the LPA trajectory offers improvement over the x^2 prediction by converging to the correct equilibrium position and including WFR, more closely matching the true

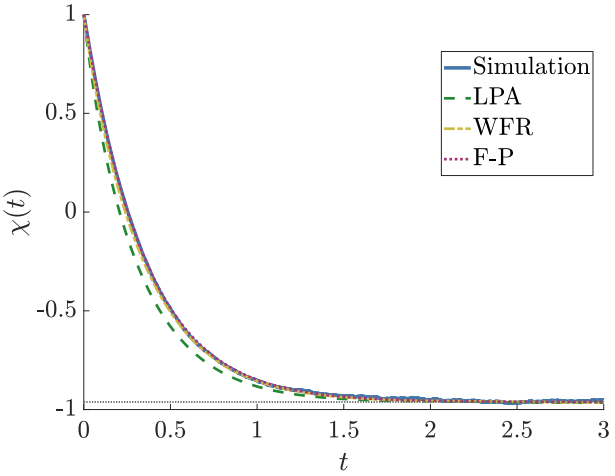

FIG. 9. The trajectory of the average position χ in a polynomial potential $\tilde{V}$ by direct simulation and solving the EEOM (108) using LPA and WFR for $\Upsilon = 10$. The horizontal dotted line is the equilibrium value.

simulated trajectory. Lowering the temperature generically decreases the accuracy of the fRG results. It is noteworthy that the fRG is able to reasonably capture these difficult dynamics well in systems where the F-P solution is difficult to obtain.

It is important to note the time advantage offered by the fRG. Solving the fRG flow equations is comparable in computation time to direct simulation while solving the F-P Eq. (34) takes longer than both. However, the latter two methods obtain solutions that are only valid for a single initial condition. A huge advantage of the fRG is that once the dynamical effective potential $\tilde{V}$ is obtained, it is trivial to solve the EEOM (108) in a couple of seconds for any initial position whereas for both direct numerical simulation of (4) and solving the F-P equation (34) one has to start again from scratch.

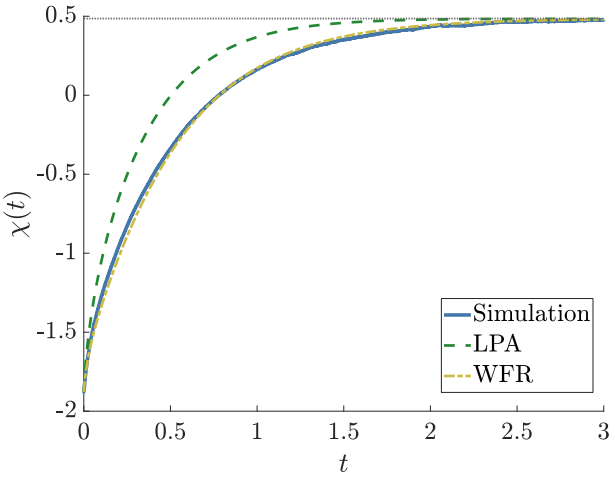

FIG. 10. The trajectory of the average position χ in a unequal LJ potential $\tilde{V}$ by direct simulation and solving the EEOM (108) using LPA and WFR for $\Upsilon = 10$. The horizontal dotted line is the equilibrium value.

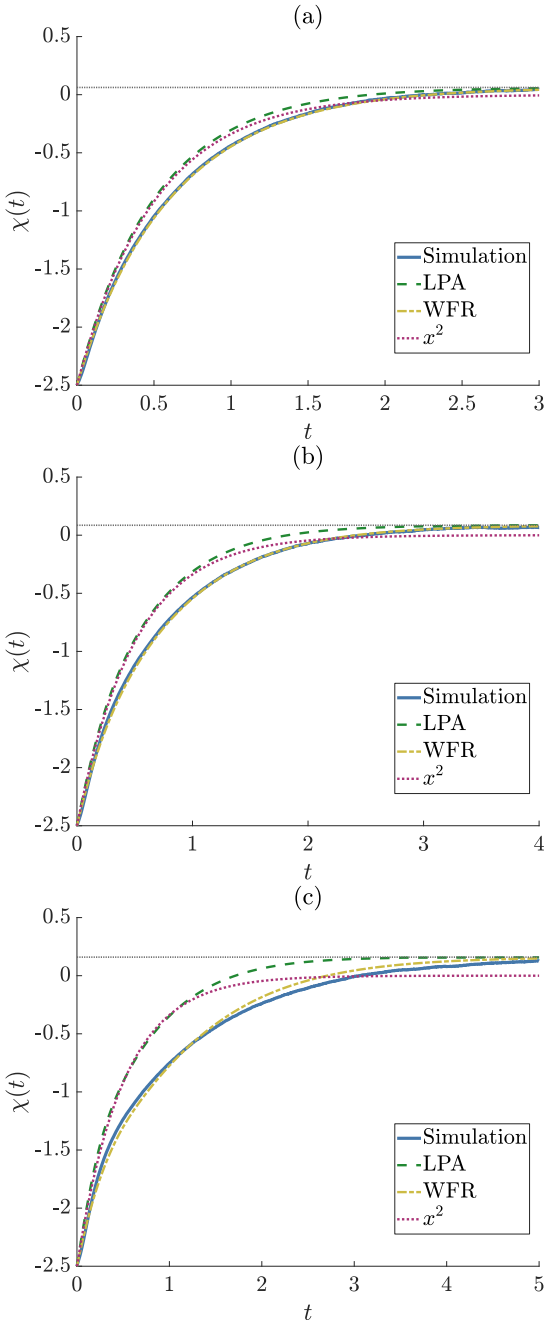

FIG. 11. The trajectory of the average position χ for x^2 potential plus six Gaussian bumps (dips) $\tilde{V}$ by direct simulation and solving the EEOM (108) using LPA and WFR for (a) $\Upsilon = 4$, (b) $\Upsilon = 3$, and (c) $\Upsilon = 2$. For comparison, the predicted evolution for the bare x^2 potential is shown by the dotted red curve. The horizontal dotted line is the equilibrium value.

C. Evolution of Var(x)

For our accelerated trajectories, we initialized the particles at the exact same point every time. This means that at $t = 0$ the probability distribution of the particles had zero variance **Var**(x) $= 0$. Using this as our initial condition, we solved numerically the EEOM for the variance (116), derived in Appendix B. In Fig. 12, we show how the variance evolves with time for the polynomial potential for $\Upsilon = 10$. We can see

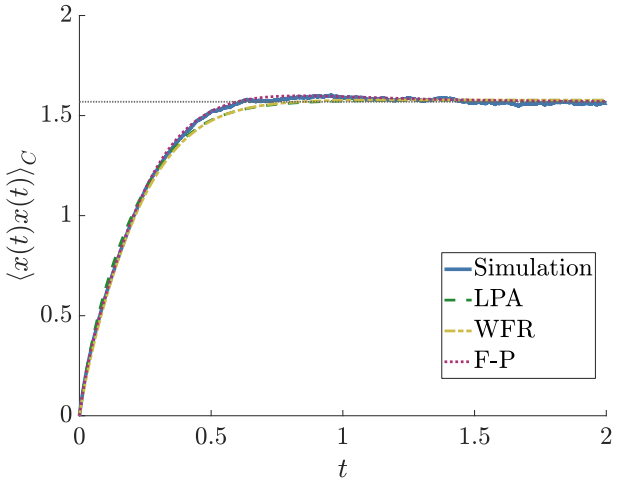

FIG. 12. The evolution of the variance **Var**(x) in a polynomial potential by direct simulation, solving the Fokker-Plank equation and solving the EEOM (116) for $\Upsilon = 10$. The horizontal dotted line is the equilibrium value.

that the LPA closely matches the numerical and F-P evolution until $t = 0.5$ before departing slightly, although it still tends toward the correct equilibrium distribution.

In Fig. 13, we show how the variance evolves with time for an unequal LJ. As with the one-point function, the F-P was unable to give sensible statistics, however, the LPA is able to very well match the early simulated trajectory, even capturing the overshooting of the variance. The WFR, on the other hand, is better at capturing the late-time decay to equilibrium.

Finally, in Fig. 14, we show how the variance evolves for the x^2 plus six Gaussian bumps (dips) potential at three different temperatures. As before, lowering the temperature decreases accuracy. In Fig. 14(c), the fRG once again clearly captures the overshooting which is a feature of the Gaussian bumps' existence; the bare x^2 evolution does not capture this behavior and overall describes the evolution poorly, converging to the wrong equilibrium variance. Again as before, the

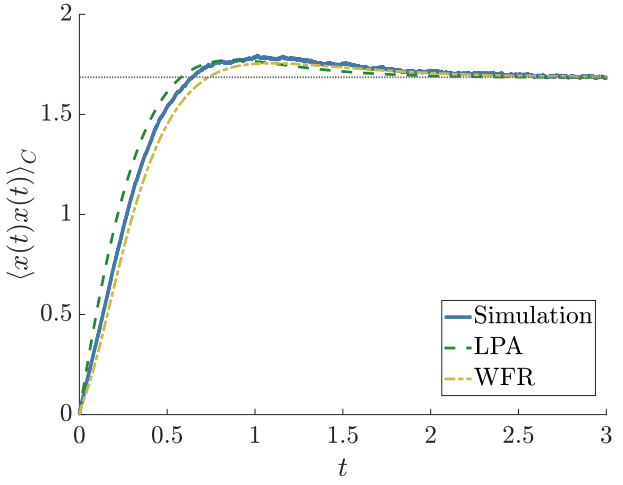

FIG. 13. The evolution of the variance **Var**(x) in an unequal LJ potential by direct simulation and solving the EEOM (116) for $\Upsilon = 10$. The horizontal dotted line is the equilibrium value.

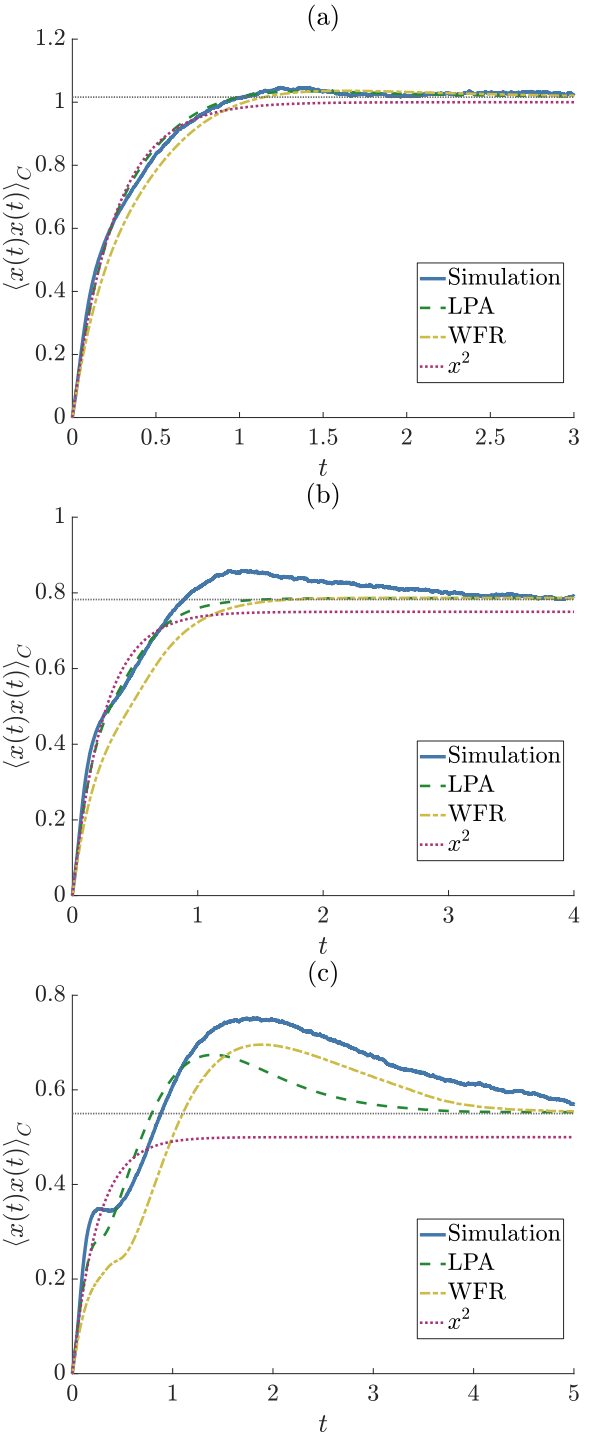

FIG. 14. The evolution of the (normalized) variance $\langle x(t)x(t)\rangle_C$ in an x^2 plus six Gaussian bumps (dips) potential for (a) $\Upsilon = 4$, (b) $\Upsilon = 3$, and (c) $\Upsilon = 2$. The horizontal dotted line is the equilibrium value.

LPA much better describes the early evolution while WFR more accurately describes late time evolution.

D. Comparison with the spectral expansion

The above results for the change in the relative performance of LPA + WFR as temperature is lowered can be

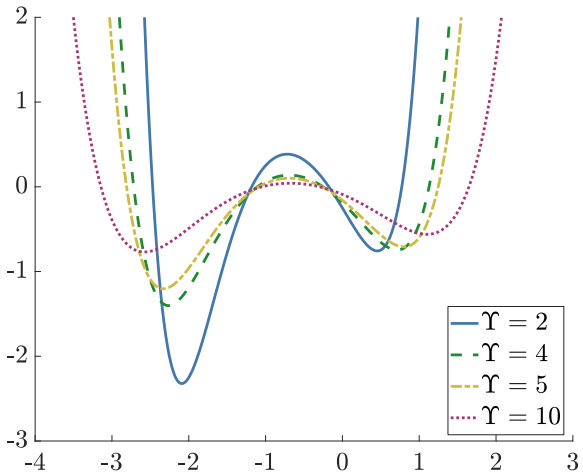

FIG. 15. The dependence of the Schrödinger potential $-\bar{U}$ (35) on the temperature Υ for the polynomial potential.

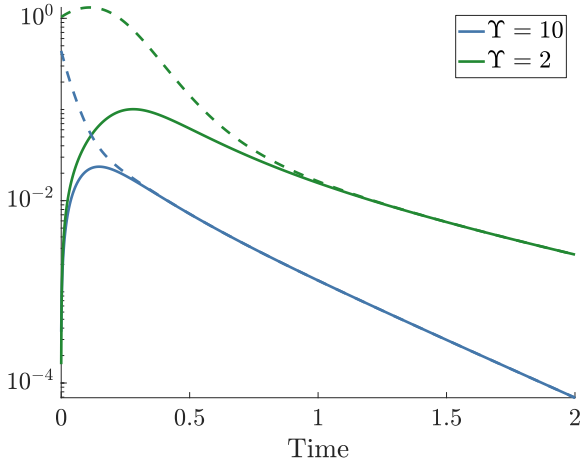

FIG. 16. The error in $\langle x^2(t)\rangle$ for a finite truncation of the spectral expansion (132) compared to the full F-P equation (34) initialized at $\chi(0) = 1$ for the polynomial potential. The dashed (solid) lines correspond to keeping the first two (50) nonzero terms. The bottom (blue) curve corresponds to $\Upsilon = 10$ and the top (green) curve to $\Upsilon = 2$.

interpreted by resorting to the spectral expansion. In Sec. II B, we recalled how all observables can be computed in a standard way from the Schrödinger-like, F-P Eq. (34) using an expansion in eigenfunctions and eigenenergies. It is straightforward to show that—given our initial conditions considered above—the average position and the two-point function can be expressed as

$$\langle x(t)\rangle = \chi_{\rm eq} + \sum_{n=1}^{\infty}\left[e^{-E_n t}e^{V(x_0)/\Upsilon}p_n(x_0) \times \int_{-\infty}^{\infty} dx\, x\, e^{-V(x)/\Upsilon}p_n(x)\right] \tag{131}$$

and

$$\langle x^2(t)\rangle = \langle x^2\rangle_{\rm eq} + \sum_{n=1}^{\infty}\left[e^{-E_n t}e^{V(x_0)/\Upsilon}p_n(x_0) \times \int_{-\infty}^{\infty} dx\, x^2\, e^{-V(x)/\Upsilon}p_n(x)\right], \tag{132}$$

where the subscript eq indicates the equilibrium value, and E_n and $p_n(x)$ are, respectively, the eigenvalues and normalized eigenfunctions of the corresponding Schrödinger-like problem. Obtaining the spectrum E_n and $p_n(x)$ may be complicated by the fact that the actual Schrödinger potential $\bar{U}$ (35) can develop temperature-dependent features as the temperature is decreased—see Fig. 15. Even for the simple polynomial potential in the Langevin equation, it is clear that at low temperatures $\bar{U}$ becomes nontrivial, developing highly asymmetrical trapping wells. The increasing energy gap between the two minima indicates that, for a fixed initial condition, higher order terms in the spectral expansion can become important as the temperature is lowered.

To illustrate the importance of these higher-order terms for the two-point function evolution in the polynomial potential, we examine the accuracy of a finite truncation of the spectral expansion at two temperatures, $\Upsilon = 10$ and $\Upsilon = 2$, for the evolution of $\langle x^2(t)\rangle$, initializing trajectories at $x = 1$: $P(x, t = 0) = \delta(x - 1)$. In Fig. 16, we plot the error associated with a finite truncation of the spectral expansion, keeping only the first two (dashed line) or 50 (solid line) terms, at two different temperatures $\Upsilon = 2$ (green, top curve) or $\Upsilon = 10$ (blue, bottom curve). This error is computed by comparing the truncated expansion to the numerical solution of the F-P equation. At early times, the error associated with keeping only two terms is larger than when 50 terms are kept, as one would expect, the discrepancy being more pronounced at lower temperatures. As the system relaxes, the contribution from the higher order terms decreases and the errors of the two truncations converge until they are essentially indistinguishable at later times, as expected. This decay of the contribution from the higher eigenvalues occurs faster for the higher temperature, making the two-term truncation more accurate earlier. This observation reinforces our inference from the previous paragraph that as temperature is lowered, higher order terms in the spectral expansion become more important for accurately describing the evolution, at least for a fixed initial condition. Crucially, this offers an explanation for why the the LPA + WFR offers poorer agreement as temperature is lowered since it would be expected to most accurately describe a circumstance where the lowest order terms in a spectral expansion dominate.

The relation between the spectral expansion and the range of validity of the EA's derivative expansion is not entirely straightforward, however, as it would also depend on the initial condition. The quantification of this relation would be an interesting undertaking which we leave for future work.

VIII. SUMMARY

Collecting results scattered in the existing literature, we have recalled how Brownian motion can be formally described by a path integral involving a Euclidean supersymmetric action and how an effective average action functional $\Gamma[\chi]$ of the average position χ, incorporating the effects of the fluctuating force and encoding all statistical properties of the process, can be calculated using fRG methods. We emphasized the

importance of utilizing the underlying symmetries of the problem, paying attention to the boundary terms which are often dropped, and showed how these can correctly incorporate any initial condition and, correspondingly, nonequilibrium evolution. The fRG flow equations were written for the first two orders of the widely used derivative expansion of the EA, referred to as the LPA and WFR. We used a particular type of regulator, the frequency-independent Callan-Symanzik regulator, for which the flow equations take on a relatively simple form, and further recalled that obtaining flow equations within the supersymmetric framework is convenient for ensuring compatibility with the Boltzmann equilibrium distribution, something that is not *a priori* obvious or guaranteed if one starts with the Onsager-Machlup form of the action (30) and considers it a Euclidean $N = 1$ scalar theory in one dimension with the Schrödinger potential $\bar{U} = \Upsilon/4\,V'' - 1/4\,(V')^2$. We also reviewed how Brownian motion can be solved using a spectral expansion method of the F-P equation in a standard way.

The EA Γ allows one to derive EEOMs for the average position $\chi(t) \equiv \langle x(t)\rangle$ and variance $\langle x^2(t)\rangle$ in an analogous manner to the classical equations of motion by taking variational derivatives. We used the LPA and WFR to compute the elements entering the EEOM, for instance, the *dynamical effective potential*. We verified the accuracy of the equilibrium limit to these equations, further emphasizing the physical significance of certain aspects of the effective potential $V_{k=0}$: namely, how the minimum of $V_{k=0}$ corresponds to the equilibrium position and its second derivative evaluated at this point to the variance through Eq. (128). We noted here that while the LPA reproduces these equilibrium quantities, the accuracy of the covariance's temporal evolution diminished as temperature was lowered.

Going beyond equilibrium, we examined how LPA + WFR handle relaxation toward it for the average position $\chi(t)$ in potentials such as a polynomial, a double well comprised of two LJ-type interactions, or a bare x^2 plus Gaussian bumps. The latter potential clearly demonstrates that the fRG is capable of capturing the effect of the nontrivial local features of this potential. In fact, the fRG could still offer reasonable approximations even in those cases where the F-P numerics failed to converge. We have also shown how the fRG can closely match the relaxation of the variance $\langle x^2(t)\rangle$ to its equilibrium value: For both the unequal LJ-type potential and the x^2 plus Gaussian bumps, the LPA variance has reasonable accuracy and still captures highly nontrivial behavior such as the variance overshooting its equilibrium value before settling to it. This is in a system where numerically solving the F-P equation failed to provide good results, at least using standard methods. Again, we find that accuracy decreases with decreasing temperature.

A clear conclusion that can be drawn from the above investigations is that decreasing the temperature negatively impacts the accuracy of using the LPA + WFR derivative expansion for the fRG to describe Brownian motion in the potentials we examined. This appears to correlate with the increasing importance at lower temperatures of higher order terms in the spectral expansion; indeed, it is expected that the lowest order terms in the derivative expansion (LPA + WFR) are best placed to describe evolution dominated by the lowest nonzero eigenvalues of the F-P spectral expansion. It would seem that the derivative expansion of the fRG for studying thermal fluctuations has utility in the range from moderate temperatures (roughly when the classical force is comparable to the noise), up to the very high temperature regime where the small local features of the potential become less relevant.

Although our conclusions on the temperature-dependent relation between the spectral expansion and the derivative expansion of the fRG are suggestive, and reasonable given the premise of the latter, a more precise quantitative comparison would be called for and should be addressed in future work. The insights gained from a more detailed, quantitative understanding of the fRG's range of validity when applied to the dynamical studies of thermally driven systems may lead to interesting and important applications. There are also issues relevant to the technicalities of applying the fRG program and which may lead to better convergence properties. For example, the recent findings of Refs. [47,48] suggest that an appropriately optimized regulator, which also excludes the regime $\omega > k$ from contributing to the flow, can ensure good convergence properties and a sizable radius of convergence. Comparisons with Refs. [47,48] are nontrivial because the supersymmetry of the Brownian motion problem makes the structure of the flow equations different to that of a simple scalar theory. This is an important question to be resolved, however, and we hope to return to it in future work.

Future work could also examine if higher order approximations beyond the WFR offer any advantage, as these might better capture higher order terms in a spectral expansion. One could further investigate an ensemble of initial conditions and try to quantify better the computational time gain the fRG offers. It is worthwhile trying to see if there is a more concrete way to determine *a priori* which systems will be well described by the fRG before having to compare to numerical simulations or doing a spectral expansion analysis. An interesting application that we didn't touch upon here might be thermal barrier escape, which in this formulation seems to be more akin to tunneling in the corresponding Euclidean quantum mechanics [49–51]; it would indeed be interesting to flesh out any analogies, if they exist. Most importantly, further understanding the application of fRG techniques to stochastically driven systems may allow extension to systems with more degrees of freedom, such as field theories and/or systems with a large number of particles. Advances in the above directions may lead to progress in theoretically tackling a broad range of physical phenomena with large separation between fundamental timescales of thermal fluctuations and long emergent timescales of macroscopic change, addressing what is now a major barrier for predictive simulations across scientific and engineering disciplines, including materials science [52], drug design [53], protein folding [54], and cosmology.

ACKNOWLEDGMENTS

A.W. would like to thank George Stagg for his numerical insight on solving the flow Eqs. (88) and (96). A.W. is funded by the EPSRC under Project No. 2120421. G.R. would like to especially thank Nikos Tetradis for very useful discussions at the early stages of this project, Julien Serreau for providing

much insight on fRG computations, and Gabriel Moreau for sharing his PhD thesis, containing many new results on the application of the fRG to the Langevin equation. We would also like to thank the referees of an earlier partial version of this paper for very useful criticisms, comments, and suggestions which helped improve it substantially, and also for bringing to our attention Refs. [47,48] and for prompting us to clarify the possible relation to Refs. [49–51].

APPENDIX A: THE EQUILIBRIUM FLOW EQUATION

In equilibrium, all equal-time expectation values can be obtained from the generating function

$$Z(J) = \int dx\, e^{-2V(x)/\Upsilon + Jx} \tag{A1}$$

in a manner directly analogous to that described in the text but with functional derivatives replaced by ordinary derivatives with respect to J. In a spirit identical to the renormalization group but in the much simpler setting of one just degree of freedom, we can define a modified generating functional [44]

$$Z_k(J) = \int dx\, e^{-2V(x)/\Upsilon - \frac{1}{2}R(k)x^2 + Jx}, \tag{A2}$$

with an additional quadratic term controlled by an arbitrary function $R(k)$ of a parameter k, satisfying $\lim_{k\to 0} R(k) = 0$, giving back the original $Z(J)$. Correlation functions are generated by $W_k(J) = \ln Z_k(J)$ via

$$\chi_k \equiv \langle x\rangle_k = \frac{\partial W_k(J)}{\partial J}, \quad \langle x^2\rangle_k - \chi_k^2 = \frac{\partial^2 W_k(J)}{\partial J^2}, \tag{A3}$$

etc. In the limit $k = 0$ and after setting $J = 0$, the usual predictions of the equilibrium Boltzmann distribution are recovered.

The source J has been considered as an external, independent variable controlling expectation values such as χ and higher correlators. One could also consider χ as the independent variable, solving $\chi = \partial W/\partial J$ for $J(\chi)$ and defining the effective potential $U(\chi)$ via a Legendre transform

$$\Gamma_k(\chi) + W_k(J) = J\chi - \tfrac{1}{2}R(k)\chi^2, \tag{A4}$$

with

$$\Gamma(\chi) \equiv 2U(\chi)/\Upsilon. \tag{A5}$$

Note that

$$\frac{\partial \Gamma_k}{\partial \chi} = J_k - R(k)\chi, \tag{A6}$$

implying that the minimum of the effective potential defines the equilibrium expectation value of x (at $J = 0$ and $k = 0$).

The dependence of the generating function $W_k(J)$ on k can be easily obtained as

$$\partial_k W_k(J) = -\frac{1}{2}\partial_k R\left[\frac{\partial^2 W_k(J)}{\partial J^2} + \left(\frac{\partial W_k(J)}{\partial J}\right)^2\right], \tag{A7}$$

which is an RG equation for $W_k(J)$. We can also obtain an equation determining how $\Gamma_k(\chi)$ runs with k. Reciprocally, taking χ as the independent variable, J becomes a function of χ and k. Taking a k derivative of (A6) at fixed χ, we obtain

$$\partial_k \Gamma_k(\chi) = \frac{1}{2}\partial_k R \frac{\partial^2 W_k}{\partial J^2} \tag{A8}$$

To express the right-hand side in terms of $\Gamma_k(\chi)$, consider the first relation of (A3). Taking a χ derivative we find

$$\left(\frac{\partial^2 \Gamma_k}{\partial \chi^2} + R\right)\frac{\partial^2 W_k}{\partial J^2} = 1. \tag{A9}$$

Hence, the RG flow of Γ is determined by

$$\partial_k \Gamma_k(\chi) = \frac{1}{2}\partial_k R\left(\frac{\partial^2 \Gamma}{\partial \chi^2} + R\right)^{-1}. \tag{A10}$$

Note also that, at $k \to 0$,

$$\langle x^2\rangle - \chi^2 = \frac{\Upsilon}{2\,\partial_\chi^2 U(\chi_{\rm eq})}, \tag{A11}$$

and hence the variance at equilibrium is determined by the curvature of the effective potential around its minimum.

All the above manipulations can be generalized to many or even infinite degrees of freedom and continuum actions, leading to the Wetterich Eq. (1), which is directly equivalent to (A10), and the relations of Sec. IV A. For this paper, it is important to note that the equilibrium effective potential $U(\chi)$ discussed here obeys the LPA flow equation *exactly* if we choose $R(k) = k$.

APPENDIX B: DERIVATION OF THE TWO POINT FUNCTION

We start from Eq. (113) repeated here for clarity,

$$\left(\frac{d^2}{dt^2} - Q(t)\right)G(t,t') = -\frac{\Upsilon}{P(t)}\delta(t-t'), \tag{B1}$$

where $Q(t) = \mathcal{U}(\chi(t))$ is given by (114) and $P(t) = 1$ or $\zeta_\chi^2(\chi(t))$ for LPA and WFR, respectively. If we now consider the homogeneous version of (B1),

$$\ddot{f}(t) - Q(t)f(t) = 0, \tag{B2}$$

it will have a growing and a decaying solution since $Q(t) > 0$, and its Wronskian $\mathcal{W}$ will simply be a constant:

$$\mathcal{W}(t) \equiv Y_1(t)\dot{Y}_2(t) - \dot{Y}_1(t)Y_2(t) = \text{const.} \tag{B3}$$

We take $Y_1(t)$ to be the growing solution and $Y_2(t)$ to be the decaying solution. Substituting the ansatz $G(t,t') = Y_1(t)F(t,t')$, where F is some function to be determined into (B1), we obtain

$$\dot{F}(t,t') = \frac{1}{Y_1^2(t)}\left[-\Upsilon\frac{Y_1(t')}{P(t')}\theta(t-t') + C_1(t')\right], \tag{B4}$$

where $\theta(t-t')$ is the Heaviside step function and $C_1(t')$ is a constant-of-integration function of t' to be determined. If we now integrate (B4), we obtain the following expression for $G(t,t')$:

$$G(t,t') = -\Upsilon\frac{Y_1(t)}{P(t')}\left[\theta(t-t')\int_{t'}^{t}\frac{Y_1(t')}{Y_1^2(u)}du + C_2(t')\right] + C_1(t')Y_1(t)\int^{t}\frac{du}{Y_1^2(u)}, \tag{B5}$$

where $C_2(t')$ is another constant-of-integration function of t' to be determined. To compute the integrals in (B5), we note

that by the definition of the Wronskian,

$$Y_1(t)\int^t \frac{\mathcal{W}(u)}{Y_1^2(u)}du = \mu Y_1(t) + Y_2(t), \tag{B6}$$

where μ is simply a constant of integration. As the Wronskian is constant here, we can simply write

$$Y_1(t)\int^t \frac{du}{Y_1^2(u)} = \frac{1}{\mathcal{W}}[\mu Y_1(t) + Y_2(t)] \tag{B7}$$

such that (B5) becomes

$$G(t,t') = \frac{\Upsilon}{\mathcal{W}P(t')}\{\bar{C}_1(t')Y_2(t) + \bar{C}_2(t')Y_1(t) + \theta(t-t')[Y_1(t)Y_2(t') - Y_1(t')Y_2(t)]\}, \tag{B8}$$

where C_1 and C_2 have been rescaled to $\bar{C}_1$ and $\bar{C}_2$ to absorb some irrelevant constant factors. We note that the functions $\bar{C}_i$ can only be linear combinations of Y_1 and Y_2,

$$\bar{C}_1(t') \equiv \alpha\, Y_1(t') + \beta\, Y_2(t'), \tag{B9}$$

$$\bar{C}_2(t') \equiv \gamma\, Y_1(t') + \delta\, Y_2(t'), \tag{B10}$$

where the constants α, β, γ, and δ will be determined later.[7] Combining all this together, we obtain the most general solution:

$$G(t,t') = \frac{\Upsilon}{\mathcal{W}P(t')}\{[\alpha - \theta(t-t')]Y_1(t')Y_2(t) + \beta\, Y_2(t')Y_2(t) + \gamma\, Y_1(t')Y_1(t) + [\delta + \theta(t-t')]Y_2(t')Y_1(t)\}. \tag{B11}$$

To obtain the values of the constants, we must now impose physical conditions:

(1) $G(t,t)$ should remain finite as $t \to \infty$, i.e., an equilibrium distribution exists at late times
$\Rightarrow \gamma = 0$.

(2) Covariance $G(t,0)$ should remain finite as $t \to \infty$
$\Rightarrow \delta = -1$.

(3) The equilibrium form of $G(t,t')$ should be symmetric under $t \leftrightarrow t'$
$\Rightarrow \alpha = 0$.

(4) Setting the initial condition to be $G(0,0) \equiv G_{00}$
$$\Rightarrow \frac{\beta\Upsilon}{\mathcal{W}} = \frac{P(0)}{Y_2(0)Y_2(0)}\left[G_{00} + Y_1(0)Y_2(0)\frac{\Upsilon}{\mathcal{W}P(0)}\right].$$

These give us the two-point function,

$$G(t,t') = \frac{\Upsilon}{2\lambda P(t')}[\theta(t-t')\tilde{Y}_1(t')\tilde{Y}_2(t) + \theta(t'-t)\tilde{Y}_2(t')\tilde{Y}_1(t)] + \frac{P(0)}{P(t')}\left[G_{00} - \frac{\Upsilon}{2\lambda P(0)}\right]\tilde{Y}_2(t')\tilde{Y}_2(t), \tag{B12}$$

where $\tilde{Y}_i(t) \equiv Y_i(t)/Y_i(0)$ and we have normalized the Wronskian as

$$\mathcal{W} = -2\lambda Y_1(0)Y_2(0), \tag{B13}$$

which is the value at equilibrium when $Q(t) \to \lambda^2$,

[7] N.B. the δ here should not to be confused with the dirac delta function.

Equation (B12) has two important limits:
The *variance* $t' \to t$,

$$\mathbf{Var}(x) \equiv G(t,t) = \frac{\Upsilon}{2\lambda P(t)}\tilde{Y}_1(t)\tilde{Y}_2(t) + \frac{P(0)}{P(t)}\left[G_{00} - \frac{\Upsilon}{2\lambda P(0)}\right]\tilde{Y}_2^2(t), \tag{B14}$$

and the *covariance* $t' \to 0, t > 0$:

$$\mathbf{Cov}(x(0)x(t)) \equiv G(t,0) = G_{00}\tilde{Y}_2(t). \tag{B15}$$

Equations (B14) and (B15) are the main results of this Appendix.

APPENDIX C: EXPLICIT COMPUTATION OF THE DETERMINANT

In this Appendix, we recall the computations of Ref. [55], explicitly showing that

$$\det \mathbf{M} = \int \mathcal{D}c\mathcal{D}\bar{c}\, \exp\left[\int dt\, \bar{c}(\partial_t + V_{,xx})c\right] \propto \exp\left[\frac{1}{2}\int dt\, V_{,xx}\right] \tag{C1}$$

when the boundary conditions

$$c(t_{\rm in}) = 0, \quad \bar{c}(t_{\rm f}) = 0 \tag{C2}$$

are chosen. We first work with the more general condition:

$$c(t_{\rm in}) = e^{-iv}c(t_{\rm f}), \quad e^{-iv}\bar{c}(t_{\rm in}) = \bar{c}(t_{\rm f}). \tag{C3}$$

From here onward, we will be working in the time interval $t \in [0,T]$ to simplify notation. Note that such a boundary condition ensures that

$$\int_0^T dt\frac{d}{dt}(\bar{c}c) = 0, \tag{C4}$$

allowing us to write

$$\det \mathbf{M} = \int \mathcal{D}c\mathcal{D}\bar{c}\, \exp\left[\frac{1}{2}\int_0^T dt\,(c,\bar{c})(0 - F^\dagger \;\; F0)(c\bar{c})\right], \tag{C5}$$

where

$$F = \partial_t + V_{,xx}, \quad F^\dagger = -\partial_t + V_{,xx}. \tag{C6}$$

Therefore, the operator in the exponent of (C5) is self-adjoint and the path integral is properly defined. The eigenfunctions and eigenvalues of F and $F^\dagger$,

$$Fu_n = \alpha_n u_n, \quad F^\dagger v_n = \alpha_n v_n, \tag{C7}$$

are

$$\alpha_n = \frac{i(2\pi n + v)}{T} + \frac{1}{T}\int_0^T d\tau V_{,xx}, \tag{C8}$$

$n = 0, \pm1, \pm2, \ldots$ and

$$u_n(t) = \frac{1}{\sqrt{T}}\exp\left\{\int_0^t d\tau(\alpha_n - V_{,xx})\right\}, \tag{C9}$$

$$v_n(t) = \frac{1}{\sqrt{T}}\exp\left\{-\int_0^t d\tau(\alpha_n - V_{,xx})\right\}. \tag{C10}$$

They form an orthonormal and complete set:

$$\int_0^T dt\ u_m(t)v_n(t) = \delta_{mn}, \tag{C11}$$

$$\sum_{n=-\infty}^{\infty} u_n(t)v_n(t') = \delta(t-t'). \tag{C12}$$

Expanding c in u_n and $\bar{c}$ in v_n with (Grassmann) coefficients b_n and $\bar{b}_n$, respectively, we can represent the determinant as

$$\det \mathbf{M} = \int \prod_{n=-\infty}^{\infty} db_n d\bar{b}_n \exp\left\{\sum_{n=-\infty}^{\infty} \alpha_n \bar{b}_n b_n\right\} = \prod_{n=-\infty}^{\infty} \alpha_n. \tag{C13}$$

Using (C8), we have

$$\prod_{n=-\infty}^{\infty} \alpha_n = \left\{\prod_{n=-\infty}^{\infty}\left(\frac{2\pi n}{T}i\right)\right\}\frac{i\nu + \int_0^T dt\, V_{,xx}}{T} \times \prod_{n=1}^{\infty}\left[1 + \frac{\left(i\nu + \int_0^T dt\, V_{,xx}\right)^2}{4\pi^2 n^2}\right], \tag{C14}$$

which gives

$$\prod_{n=-\infty}^{\infty} \alpha_n = \frac{2\prod_{n=-\infty}^{\infty}\left(\frac{2\pi n}{T}i\right)}{T} \sinh\left[\frac{1}{2}\left(i\nu + \int_0^T dt\, V_{,xx}\right)\right]. \tag{C15}$$

With the infinite constant absorbed in the definition of the path integral measure, the choice $\nu \to -i\infty$ gives the required result 20. Note that other, perhaps more obvious choices, e.g., periodic ($\nu = 0$) or antiperiodic ($\nu = \pi$) boundary conditions, do not reproduce the determinant which corresponds to the causal stochastic problem.

[1] N. G. Van Kampen, *Stochastic Processes in Physics and Chemistry* (Elsevier, Amsterdam, The Netherlands, 2007).

[2] C. Gardiner, *Stochastic Methods* (Springer, Berlin, Heidelberg, 2009), Vol. 4.

[3] A. A. Starobinsky and J. Yokoyama, Equilibrium state of a self-interacting scalar field in the de Sitter background, Phys. Rev. D **50**, 6357 (1994).

[4] C. Wetterich, Exact evolution equation for the effective potential, Phys. Lett. B **301**, 90 (1993).

[5] T. R. Morris, The exact Renormalization group and approximate solutions, Int. J. Mod. Phys. A **09**, 2411 (1994).

[6] J. Berges, N. Tetradis, and C. Wetterich, Non-perturbative renormalization flow in quantum field theory and statistical physics, Phys. Rep. **363**, 223 (2002).

[7] N. Dupuis, L. Canet, A. Eichhorn, W. Metzner, J. M. Pawlowski, M. Tissier, and N. Wschebor, The nonperturbative functional renormalization group and its applications, Phys. Rep. **910**, 1 (2021).

[8] H. Gies, Introduction to the functional RG and applications to gauge theories, Lect. Notes Phys. **852**, 287 (2012).

[9] B. Delamotte, An introduction to the nonperturbative renormalization group, Lect. Notes Phys. **852**, 49 (2012).

[10] K. G. Wilson, The renormalization group and critical phenomena, Rev. Mod. Phys. **55**, 583 (1983).

[11] M. E. Peskin and D. V. Schroeder, *An Introduction to Quantum Field Theory* (Addison-Wesley, Reading, 1995).

[12] P. M. Chaikin and T. C. Lubensky, *Principles of Condensed Matter Physics* (Cambridge University Press, Cambridge, 1995).

[13] A. Vasil'ev, *The Field Theoretic Renormalization Group in Critical Behavior Theory and Stochastic Dynamics* (Chapman and Hall/CRC, London, 2004).

[14] G. Parisi and N. Sourlas, Supersymmetric field theories and stochastic differential equations, Nucl. Phys. B **206**, 321 (1982).

[15] J. Zinn-Justin, *Quantum Field Theory and Critical Phenomena*, International Series of Monographs on Physics (Clarendon Press, Oxford, 2002).

[16] F. Synatschke, G. Bergner, H. Gies, and A. Wipf, Flow equation for supersymmetric quantum mechanics, J. High Energy Phys. 03 (2009) 028.

[17] A. Vasiliev, *Functional Methods in Quantum Field Theory and Statistical Physics* (CRC Press, London, 1998).

[18] C. De Dominicis, Techniques de renormalization de la Théorie des Champs Et Dynamique Des Phénomènes Critiques, J. Phys. Colloq. **37**, C1-247 (1976).

[19] H.-K. Janssen, On a Lagrangean for classical field dynamics and renormalization group calculations of dynamical critical properties, Z. Physik B: Condensed Matter **23**, 377 (1976).

[20] C. De Dominicis and L. Peliti, Field-theory renormalization and critical dynamics above T_c : Helium, antiferromagnets, and liquid-gas systems, Phys. Rev. B **18**, 353 (1978).

[21] P. C. Martin, E. D. Siggia, and H. A. Rose, Statistical dynamics of classical systems, Phys. Rev. A **8**, 423 (1973).

[22] A. W. Lau and T. C. Lubensky, State-dependent diffusion: Thermodynamic consistency and its path integral formulation, Phys. Rev. E: Stat., Nonlinear, Soft Matter Phys. **76**, 011123 (2007).

[23] J. A. Hertz, Y. Roudi, and P. Sollich, Path integral methods for the dynamics of stochastic and disordered systems, J. Phys. A: Math. Theor. **50**, 033001 (2017).

[24] T. Markkanen, A. Rajantie, S. Stopyra, and T. Tenkanen, Scalar correlation functions in de Sitter space from the stochastic spectral expansion, J. Cosmol. Astropart. Phys. 08 (2019) 001.

[25] H. Leschke and M. Schmutz, Operator orderings and functional formulations of quantum and stochastic dynamics, Z. Physik B: Condensed Matter **27**, 85 (1977).

[26] K. Mallick, M. Moshe, and H. Orland, A field-theoretic approach to non-equilibrium work identities, J. Phys. A: Math. Theor. **44**, 095002 (2011).

[27] P. H. Damgaard and H. Hüffel, Stochastic quantization, Phys. Rep. **152**, 227 (1987).

[28] L. Canet, B. Delamotte, O. Deloubrière, and N. Wschebor, Nonperturbative Renormalization-Group Study of Reaction-Diffusion Processes, Phys. Rev. Lett. **92**, 195703 (2004).

[29] R. Gezzi, T. Pruschke, and V. Meden, functional renormalization group for nonequilibrium quantum many-body problems, Phys. Rev. B **75**, 045324 (2007).
[30] S. G. Jakobs, V. Meden, and H. Schoeller, Nonequilibrium Functional Renormalization Group for Interacting Quantum Systems, Phys. Rev. Lett. **99**, 150603 (2007).
[31] T. Gasenzer and J. M. Pawlowski, Towards far-from-equilibrium quantum field dynamics: A functional renormalization-group approach, Phys. Lett. B **670**, 135 (2008).
[32] J. Berges and G. Hoffmeister, Nonthermal fixed points and the functional renormalization group, Nucl. Phys. B **813**, 383 (2009).
[33] T. Gasenzer, S. Keßler, and J. M. Pawlowski, Far-from-equilibrium quantum many-body dynamics, Eur. Phys. J. C **70**, 423 (2010).
[34] T. Kloss and P. Kopietz, Nonequilibrium time evolution of bosons from the functional renormalization group, Phys. Rev. B **83**, 205118 (2011).
[35] L. Canet, H. Chaté, and B. Delamotte, General framework of the non-perturbative renormalization group for non-equilibrium steady states, J. Phys. A: Math. Theor. **44**, 495001 (2011).
[36] L. M. Sieberer, S. D. Huber, E. Altman, and S. Diehl, Nonequilibrium functional renormalization for driven-dissipative Bose-Einstein condensation, Phys. Rev. B **89**, 134310 (2014).
[37] S. Mukherjee, R. Venugopalan, and Y. Yin, Real-time evolution of non-Gaussian cumulants in the QCD critical regime, Phys. Rev. C **92**, 034912 (2015).
[38] J. M. Pawlowski and N. Strodthoff, Real time correlation functions and the functional renormalization group, Phys. Rev. D **92**, 094009 (2015).
[39] L. Corell, A. K. Cyrol, M. Heller, and J. M. Pawlowski, Flowing with the Temporal renormalization Group, Phys. Rev. D **104**, 025005 (2021).
[40] C. Duclut and B. Delamotte, Frequency regulators for the non-perturbative renormalization group: A general study and the model A as a benchmark, Phys. Rev. E **95**, 012107 (2017).
[41] G. Moreau and J. Serreau, Unequal time correlators of stochastic scalar fields in de Sitter space, Phys. Rev. D **101**, 045015 (2020).
[42] T. Prokopec and G. Rigopoulos, Functional renormalization group for stochastic inflation, J. Cosmol. Astropart. Phys. **2018**, 013 (2018).
[43] G. Moreau, Nonperturbative dynamics of quantum fields in de Sitter spacetime, Ph.D. thesis, APC Paris, 2020.
[44] M. Guilleux and J. Serreau, Quantum scalar fields in de Sitter space from the nonperturbative renormalization group, Phys. Rev. D **92**, 084010 (2015).
[45] M. Guilleux and J. Serreau, Nonperturbative renormalization group for scalar fields in de Sitter space: Beyond the local potential approximation, Phys. Rev. D **95**, 045003 (2017).
[46] T. Markkanen and A. Rajantie, Scalar correlation functions for a double-well potential in de Sitter space, J. Cosmol. Astropart. Phys. 03 (2020) 049.
[47] I. Balog, H. Chaté, B. Delamotte, M. Marohnić, and N. Wschebor, Convergence of Nonperturbative Approximations to the Renormalization Group, Phys. Rev. Lett. **123**, 240604 (2019).
[48] G. De Polsi, I. Balog, M. Tissier, and N. Wschebor, Precision calculation of critical exponents in the O(N) universality classes with the nonperturbative renormalization group, Phys. Rev. E **101**, 042113 (2020).
[49] A. Strumia and N. Tetradis, A consistent calculation of bubble-nucleation rates, Nucl. Phys. B **542**, 719 (1999).
[50] A. Strumia and N. Tetradis, Bubble-nucleation rates for radiatively induced first-order phase transitions, Nucl. Phys. B **554**, 697 (1999).
[51] A. Strumia, N. Tetradis, and C. Wetterich, The region of validity of homogeneous nucleation theory, Phys. Lett. B **467**, 279 (1999).
[52] S. Yip and M. P. Short, Multiscale materials modelling at the mesoscale, Nat. Mater. **12**, 774 (2013).
[53] M. C. Zwier and L. T. Chong, Reaching biological timescales with all-atom molecular dynamics simulations, Current Opinion Pharmacology **10**, 745 (2010).
[54] P. L. Freddolino, C. B. Harrison, Y. Liu, and K. Schulten, Challenges in protein-folding simulations, Nat. Phys. **6**, 751 (2010).
[55] S. Marculescu, K. Okano, and L. Schulke, Superspace renormalization and stochastic quantization, Nucl. Phys. B **349**, 463 (1991).